0026-895X/99/030619-14$3.00/0

MOLECULAR PHARMACOLOGY, **56:**619–632 (1999).

N-methyl-D-aspartate Excitotoxicity: Relationships among Plasma Membrane Potential, Na^+/Ca^{2+} Exchange, Mitochondrial Ca^{2+} Overload, and Cytoplasmic Concentrations of Ca^{2+}, H^+, and K^+

LECH KIEDROWSKI

The Psychiatric Institute, Departments of Psychiatry and Pharmacology, College of Medicine, The University of Illinois at Chicago, Chicago, Illinois

Received December 7, 1998; accepted June 9, 1999

This paper is available online at http://www.molpharm.org

ABSTRACT

A high cytoplasmic Na^+ concentration may contribute to *N*-methyl-D-aspartate (NMDA)-induced excitotoxicity by promoting Ca^{2+} influx via reverse operation of the Na^+/Ca^{2+} exchanger (NaCaX), but may simultaneously decrease the electrochemical Ca^{2+} driving force by depolarizing the plasma membrane (PM). Digital fluorescence microscopy was used to compare the effects of Na^+ versus ions that do not support the NaCaX operation, i.e., *N*-methyl-D-glucamine$^+$ or Li^+, on: PM potential; cytoplasmic concentrations of Ca^{2+}, H^+, and K^+; mitochondrial Ca^{2+} storage; and viability of primary cultures of cerebellar granule cells exposed to NMDA receptor agonists. In the presence of Na^+ or Li^+, NMDA depolarized the PM and decreased cytoplasmic pH (pH_C); in the presence of Li^+, Ca^{2+} influx was reduced, mitochondrial Ca^{2+} overload did not occur, and the cytoplasm became more acidified than in the presence of Na^+. In the presence of *N*-methyl-D-glucamine$^+$, NMDA instantly hyperpolarized the PM, but further changes in PM potential and pH_C were Ca-dependent. In the absence of Ca^{2+}, hyperpolarization persisted, pH_C was decreasing very slowly, K^+ was retained in the cytoplasm, and cerebellar granule cells survived the challenge; in the presence of Ca^{2+}, pH_C dropped rapidly, the K^+ concentration gradient across the PM began to collapse as the PM began to depolarize, and Ca^{2+} influx and excitotoxicity greatly increased. These results indicate that the dominant, very likely excitotoxic, component of NMDA-induced Ca^{2+} influx is mediated by reverse NaCaX and that direct Ca^{2+} influx via NMDA channels is curtailed by Na-dependent PM depolarization.

Excitotoxicity has been causally linked with glutamate-elicited Ca^{2+} influx (Choi, 1987; Hartley et al., 1993; Eimerl and Schramm, 1994) and with Ca^{2+} accumulation in mitochondria (Kiedrowski and Costa, 1995; White and Reynolds, 1996; Schinder et al., 1996; Stout et al., 1998). Although exposure to glutamate also greatly elevates cytoplasmic Na^+ concentrations ($[Na^+]_C$) in cultured neurons (Kiedrowski et al., 1994; Pinelis et al., 1994), it is yet unclear what role the increase in $[Na^+]_C$ plays in excitotoxicity. Although excessive swelling caused by the influx of Na^+, Cl^-, and water leads to neuronal death (Rothman, 1985; Choi, 1987), such a mechanism characterizes kainate- rather than glutamate- or NMDA-induced excitotoxicity (Kiedrowski, 1998). Earlier studies have shown that high $[Na^+]_C$ contributes to the NMDA-induced Ca^{2+} influx by activating the reverse operation of the plasma membrane Na^+/Ca^{2+} exchanger (NaCaX) (Kiedrowski et al., 1994; Hoyt et al., 1998). The activation of the reverse NaCaX also requires that cytoplasmic Ca^{2+} be raised to micromolar levels (Hilgemann et al., 1992). This makes the channels that are permeable for both Na^+ and Ca^{2+}, such as NMDA receptor channels (Mayer and Westbrook, 1987), perfect triggers of the reverse NaCaX activation.

The role of the NaCaX in excitotoxicity was previously tested in vitro using Na-free media (Mattson et al., 1989; Storozhevykh et al., 1998) in which Na^+ was substituted

This work was supported in part by National Institutes of Health Grant NS 37390 and presented in part in abstract form, Society of Neuroscience Abstracts 300.5, 1998.

ABBREVIATIONS: $[Na^+]_C$, $[K^+]_C$, and $[Ca^{2+}]_C$, cytoplasmic concentrations of Na^+, K^+, and Ca^{2+}, respectively; BCECF, 2′,7′-bis-(2-carboxyethyl)-5-(and-6)-carboxyfluorescein; CaDF, electrochemical force for Ca^{2+} influx; CGCs, cerebellar granule cells; CM, conditioned medium; $DiBAC_4(3)$, bis(1,3-dibutylbarbituric acid)trimethine oxonol; E_m, plasma membrane potential; $[K^+]_E$, extracellular concentration of K^+; Li-L, NMG-L, Cs-L, Na-free Locke's buffers in which Na^+ was substituted with Li^+, NMG^+, or Cs^+, respectively; MDC, mitochondria-depolarizing cocktail; NaCaX and NaHX, Na^+/Ca^{2+} and Na^+/H^+ exchanger, respectively; Na-L, standard Locke's buffer containing physiological Na^+ concentrations; nF_{488}, normalized fluorescence emitted by $DiBAC_4(3)$ after excitation at 488 nm; NMDA, *N*-methyl-D-aspartate; NMG^+, *N*-methyl-D-glucamine$^+$; PBFI, K^+-binding benzofuran isophthalate; pH_C, cytoplasmic pH; PM, plasma membrane.

with a large cation, *N*-methyl-D-glucamine (NMG^+), that very poorly, if at all, permeates NMDA receptor channels. These studies showed that in the presence of NMG^+, the NMDA-induced Ca^{2+} influx and excitotoxicity are greatly enhanced, and the data were interpreted as indicating that such an outcome results from an inhibition of Ca^{2+} extrusion by the NaCaX (Mattson et al., 1989), or from an alleged excessive release of endogenous glutamate (Storozhevykh et al., 1998). Because these interpretations failed to consider that the substitution of Na^+ with NMG^+ might prevent the Na-dependent plasma membrane (PM) depolarization that normally accompanies activation of NMDA receptors, the aim of the present study was to test what impact such depolarization has on the NMDA-induced Ca^{2+} influx and excitotoxicity.

To this end, using digital fluorescence microscopy and fluorophores sensitive to the plasma membrane potential (E_m) and to cytoplasmic Ca^{2+} concentrations ($[Ca^{2+}]_C$), E_m, and $[Ca^{2+}]_C$ were simultaneously monitored in primary cultures of cerebellar granule cells (CGCs) exposed to NMDA. NMDA receptors were activated by an agonist, whereas extracellular Na^+ was present or substituted either with NMG^+ or with Li^+. Because neither NMG^+ nor Li^+ support Ca^{2+} transport via the NaCaX (Blaustein, 1977; Hilgemann 1989), but Li^+, in contrast to NMG^+, permeates NMDA receptor channels (Tsuzuki et al., 1994) and should depolarize the PM (Hösli et al., 1973), this experimental design was expected to isolate the effects of PM depolarization from the effects of Na-dependent activation of the NaCaX. Because substitution of extracellular Na^+ with Li^+ or NMG^+ is also expected to affect the operation of the plasma membrane Na^+/H^+ exchanger (NaHX), which controls cytoplasmic pH (pH_C) (Aronson, 1985), and because the role of pH_C in Ca^{2+} homeostasis is obscure, pH_C was also monitored.

Materials and Methods

Neuronal Cultures. CGCs were prepared from 8-day-old Sprague-Dawley rats and suspended in culture medium consisting of basal Eagle's medium supplemented with 25 mM KCl, 10% bovine fetal serum, 2 mM glutamine, and 50 μg/ml gentamycin, as described previously (Kiedrowski et al., 1994). The cells were plated on poly-D-lysine (10 μg/ml)-coated 35-mm dishes at a density of 2×10^6 cells/dish; for the imaging experiments, CGCs were plated on poly-D-lysine-coated 2.5-cm glass coverslips. Glial proliferation was curtailed by the addition of 10 μM cytosine arabinofuranoside 24 h after plating. Cultures at 8 to 11 days in vitro were used for the experiments.

Media. Experimental solutions were based on Locke's buffer (Na-Locke's) containing 154 mM NaCl, 5.6 mM KCl, 3.6 mM $NaHCO_3$, 1.3 mM $CaCl_2$, 1 mM $MgCl_2$, 5 mM glucose, and 10 mM HEPES, pH 7.4, adjusted with Tris. The Na-free Locke's buffer in which Na^+ was replaced with Li^+ (Li-Locke's) contained 157.6 mM LiCl, 2 mM KCl, and 3.6 mM $KHCO_3$, with the remaining ingredients the same as in Na-Locke's. When Na^+ was replaced with NMG^+ or Cs^+, the buffer was identical with Li-Locke's except that Li^+ was substituted with NMG^+ or Cs^+, respectively. Ca-free solutions contained 3 mM EGTA and no $CaCl_2$, with other components of Locke's buffer unchanged. Glutamate (100 μM) or NMDA (300 μM) were applied in Mg-free media containing 10 μM glycine. Glucose-free solutions contained 5 mM 2-deoxy-D-glucose instead of D-glucose. The mitochondria-depolarizing cocktail (MDC) was composed of a Ca- and glucose-free Na-Locke's supplemented with 10 μM cyanide *m*-chlorophenylhydrazone (CCCP), 3 μg/ml oligomycin, and 10 μM MK-801 [(+)5-methyl-10–11-dihydro-5H-dibenzocyclohepten-5,10-imine].

Viability Test. $[Ca^{2+}]_C$ levels were monitored in CGCs exposed to glutamate as described in the text. Following glutamate withdrawal, by washing with Na-Locke's, $[Ca^{2+}]_C$ levels were monitored for an additional 20 to 30 min. Then the cells were returned to a conditioned medium (CM), i.e., the medium (containing 25 mM KCl) in which the cells were cultured. Viability of the same cells was assessed after 20 to 24 h by comparing oblique illumination images of the neurons occupying the same microscopic field before and 20 to 24 h after the excitotoxic challenge; neurons with a damaged PM were identified using propidium iodide (Jones and Senft, 1985). To this end, the cells were incubated for about 10 min at room temperature with 10 μM propidium iodide dissolved in Na-Locke's, and the propidium iodide fluorescence emitted at over 520 nm after 488 nm excitation was imaged. Whether the positions of propidium iodide-positive spots corresponded to the positions of dead cells was examined by digitally subtracting, using the Attofluor software (Atto Instruments, Rockville, MD), the images of the propidium fluorescence from the oblique illumination images of the same microscopic field. This procedure allows one to distinguish false signals, i.e., the propidium iodide-positive spots representing cellular debris floating in the medium. In some experiments propidium iodide was added to the CM immediately after the challenge with glutamate, and the progression of the plasma membrane deterioration was followed for up to 70 h by monitoring the propidium iodide fluorescence.

Simultaneous Assay of $[Ca^{2+}]_C$ and E_m. The coverslips plated with CGCs were transferred to custom-made recording chambers, in which the cells were loaded for 60 min at 37°C with 4 μM of fura-2 acetoxymethyl ester dissolved in CM. The stock concentration of fura-2 acetoxymethyl ester was 1 mM, in dimethyl sulfoxide (DMSO). Following the loading, the cells were washed using CM without fura-2. Fluorescence data were acquired from the cells that, based on their neuronal appearance and the small size of the cell bodies (about 10 μm in diameter), could be identified as CGCs. Occasionally, larger cells (about 20 μm in diameter), most likely astrocytes, were also observed and monitored. All imaging experiments were carried out at 37°C using the TC-102 temperature controller and the LU-CB1 Leiden culture system from Medical Systems Corp. (Greenvale, NY). Monitoring of the fura-2 fluorescence was begun while the cells were still incubated in CM; the pH of the CM was maintained at physiological levels by delivering 6% CO_2 to the recording chamber. Then, the CM in the recording chamber was replaced with Na-Locke's supplemented with 100 nM bis(1,3-dibutylbarbituric acid)trimethine oxonol [$DiBAC_4(3)$] to monitor E_m (Bräuner et al., 1984; Laskey et al., 1992).

The fura-2 and the $DiBAC_4(3)$ fluorescences were monitored using the Attofluor digital imaging system, Zeiss Axiovert 10 microscope (Carl Zeiss, Thornwood, NY), and Zeiss Achrostigmat 40×, NA 1.30, objective. The images of fluorescence emitted at over 520 nm after excitation at 334 nm (F_{334}) and 380 nm (F_{380}) for fura-2, and at 488 nm (F_{488}) for $DiBAC_4(3)$ were saved every 10 to 20 s. The fluorescence intensities, measured in selected regions of interest, were analyzed retroactively. To display fura-2 and $DiBAC_4(3)$ distribution within single cells, using Adobe Photoshop 4.0, the superimposed images of fura-2 and $DiBAC_4(3)$ fluorescence were created by transferring 8-bit gray scale images of fura-2 fluorescence ($F_{334} + F_{380}$) and $DiBAC_4(3)$ fluorescence (F_{488}) to red and green channels, respectively, of a 24-bit RGB (red-green-blue) image.

The $DiBAC_4(3)$ fluorescence measured in regions of interest positioned in the peripheral parts of neuronal somata was used as a relative index of E_m. To normalize this fluorescence among various neurons, at the end of the experiments, the cells were depolarized using the following solution in which chloride was partially replaced with gluconate to prevent cell swelling: 5 μM gramicidin D, 134.2 mM K-gluconate, 25.4 mM KCl, 1.3 mM $CaCl_2$, 1 mM $MgCl_2$, 3.6 mM $KHCO_3$, and 10 mM HEPES, pH 7.2, adjusted with Tris; this exposure caused an increase in F_{488} to a value representing the maximal depolarization ($maxF_{488}$). The F_{488} in the background ($bckgF_{488}$) was

measured in cell-free areas. The normalized F_{488} (nF_{488}) was calculated according to the formula:

$$nF_{488} = (F_{488} - bckgF_{488})/(maxF_{488} - bckgF_{488}).$$

$[Ca^{2+}]_C$ calibration was performed in situ. The minimal F_{334}/F_{380} ratio (R_{min}) was measured in CGCs incubated for up to 30 min in a buffer containing 10 μM ionomycin, 5 mM EGTA, 154 mM NaCl, 5.6 mM KCl, 1 mM $MgCl_2$, 3.6 mM $NaHCO_3$, 5 mM glucose, and 10 mM HEPES, pH 7.4. The maximal F_{334}/F_{380} ratio (R_{max}) was measured at the end of the experiments by exposing the cells to 10 μM ionomycin, 10 μM CCCP, 134.2 mM K-gluconate, 25.4 mM KCl, 5 mM $CaCl_2$, 1 mM $MgCl_2$, 3.6 mM $KHCO_3$, 10 mM HEPES, pH 7.2, adjusted with Tris; after 5 to 10 min, a stable F_{334}/F_{380} ratio was reached, which was assumed to represent R_{max}. The in situ calibration procedure also determined the ratio (β) of the fluorescence emitted at 380 nm by fura-2-Ca-free versus fura-2-Ca-saturated. R_{max}, R_{min}, β, and the association constant of fura-2 and Ca^{2+}, of 224 nM, were used to calculate $[Ca^{2+}]_C$ as described by Grynkiewicz et al. (1985). The background F_{334} and F_{380} values were measured in cell-free areas at all time points of the experiments. When the F_{334}/F_{380} ratio data were calibrated for $[Ca^{2+}]_C$ with background subtraction, the average $[Ca^{2+}]_C$ values did not differ by more than 10% from the values calculated without background subtraction. The data noise during the R_{max} data acquisition, was greatly increased, however, when the background subtraction was performed (data not shown). This increase in the R_{max} data noise was due to the fact that the background subtraction procedure greatly increased the variability of the already very low F_{380} values recorded during the R_{max} acquisition. Because the effect of the background subtraction procedure on the calculated $[Ca^{2+}]_C$ values was small and might have resulted from the increased noise of the F_{380} data, the $[Ca^{2+}]_C$ values presented in this report were calculated without background subtraction.

Simultaneous Assay of $[Ca^{2+}]_C$ and pH_C. The coverslips with CGCs were handled the same way as described above for the assay of $[Ca^{2+}]_C$ and E_m except that the cells were loaded for 60 min at 37°C with 4 μM fura-2 acetoxymethyl ester plus 0.2 μM BCECF (2′,7′-bis-(2-carboxyethyl)-5-(and-6)-carboxyfluorescein) acetoxymethyl ester. The stock concentration of BCECF acetoxymethyl ester was 0.05 mM, in DMSO. Following the loading, the cells were washed using CM without fura-2 and BCECF. Images of the fluorescence emitted at over 520 nm at 334, 380, 440, and 488 nm excitations were saved every 10 to 20 s. $[Ca^{2+}]_C$ was calculated from the F_{334}/F_{380} ratio as described earlier. The F_{488}/F_{440} ratio was used to determine pH_C from the in situ calibrations performed after each experiment. The background F_{440} and F_{488} values were measured in cell-free areas at all time points and were subtracted from the fluorescence data before calculating the F_{488}/F_{440} ratio. The pH calibrating solutions contained 10 μM nigericin, 10 μM CCCP, 134.2 mM K-gluconate, 25.4 mM KCl, 1.3 mM $CaCl_2$, 1 mM $MgCl_2$, 3.6 mM $KHCO_3$, and 10 mM 2-[*N*-morpholino]ethanesulfonic acid or 10 mM HEPES. 2-[*N*-morpholino]ethanesulfonic acid was used to adjust the pH of the calibrating solution to a range of 5.5 to 6.5; HEPES was used in the pH range of 7.0 to 8.0. The data were fitted to the four-parameter equation of a sigmoidal curve:

$$F_{488}/F_{440}\ \text{ratio} = y_0 + a/(1 + \exp(-(pH - x_0)/b)).$$

Representative experiments ($n = 7$) yielded the following parameters: $y_0 = 0.39 \pm 0.01$, $a = 1.18 \pm 0.06$, $x_0 = 6.99 \pm 0.03$, and $b = 0.41 \pm 0.02$.

Assay of Cytoplasmic K^+ Concentration ($[K^+]_C$). CGCs were loaded for 60 min at 37°C with 5 μM K^+ binding benzofuran isophthalate (PBFI) acetoxymethyl ester dissolved in CM. The stock concentration of PBFI acetoxymethyl ester was 1.25 mM, in DMSO. PBFI fluorescence was monitored at 37°C using the same excitation and emission settings as described for fura-2. The F_{334}/F_{380} ratio was calibrated for $[K^+]_C$ in situ at the end of the experiments. The $[K^+]_C$ calibrating buffers were prepared by appropriate mixing of two solutions containing high and low concentrations of K^+. The high-concentration K^+ solution contained 5 μM gramicidin D, 134.2 mM K-gluconate, 25.4 mM KCl, 3.6 mM $KHCO_3$, 1 mM $MgCl_2$, and 10 mM HEPES, pH 7.2, adjusted with Tris. In the low-concentration K^+ solution, 134.2 mM Li-gluconate and 25.4 mM LiCl were used instead of the respective K^+ salts, and the remaining ingredients were unchanged. $[K^+]_C$ values were calculated using a nonlinear least-squares fit of the data to the Michaelis-Menten equation as described by Kasner and Ganz (1992).

$^{45}Ca^{2+}$ Uptake. CGCs were incubated for 15 min at 37°C with 1 ml of experimental media containing 1 μCi of $^{45}Ca^{2+}$. The extracellular $^{45}Ca^{2+}$ was then removed by triple washing with 2 ml of an ice-cold buffer that contained 154 mM NaCl, 5.6 mM KCl, 3.6 mM $NaHCO_3$, 1 mM $MgCl_2$, 2 mM EGTA, and 10 mM HEPES, pH 7.4, adjusted with Tris. The cells were then dissolved in 1 ml of 0.5 M NaOH; neutralized aliquots of this solution were used for scintillation spectroscopy and for protein determination.

Statistical Analysis. All averaged data are expressed as the means ± S.E.M. The statistical tests used are indicated in the text. All statistical analyses of the $[Ca^{2+}]_C$ data were performed using the F_{334}/F_{380} ratios. The $[Ca^{2+}]_C$ data could not be used for statistical analysis because when $[Ca^{2+}]_C$ approached the fura-2 saturating levels, the calculated $[Ca^{2+}]_C$ values became very imprecise. In some experiments, the fura-2 fluorescence was monitored using different sets of neutral density filters and/or gains, which affected the absolute values of the F_{334}/F_{380} ratios (for example, note the differences in F_{334}/F_{380} ratios between Figs. 2 and 6). To normalize the data, the F_{334}/F_{380} ratios were converted to $[Ca^{2+}]_C$ values using the calibrating parameters R_{max}, R_{min}, and β obtained in sister cultures in the same experimental sessions; then, the $[Ca^{2+}]_C$ values from various experiments were converted to the normalized F_{334}/F_{380} ratio using a single representative set of the calibrating parameters R_{max}', R_{min}', and β', according to the formula:

$$\text{normalized } F_{334}/F_{380}\ \text{ratio} = \frac{([Ca^{2+}]_c \times R_{max}') + (\beta' \times R_{min}')}{[Ca^{2+}]_c + \beta'}.$$

Materials. Fura-2 acetoxymethyl ester, PBFI acetoxymethyl ester, BCECF acetoxymethyl ester, and $DiBAC_4(3)$ were obtained from Molecular Probes (Eugene, OR). MK-801 was purchased from Research Biochemicals Inc. (Natick, MA). The culture media and all other chemicals were from Sigma Chemical Co. (St. Louis, MO).

Results and Discussion

$[Ca^{2+}]_C$ Levels in CGCs Incubated in CM. Although the very low (about 20 nM) $[Ca^{2+}]_C$ levels in CGCs incubated in Na-Locke's are very homogeneous, a small number of CGCs show a marked heterogeneity in glutamate-induced $[Ca^{2+}]_C$ transients and fail to efficiently buffer cytoplasmic Ca^{2+} (see Fig. 4C in Kiedrowski and Costa, 1995). In the present study, it was routinely observed that it is possible to predict which neurons will fail to buffer the glutamate-induced $[Ca^{2+}]_C$ transients. From among 1713 CGCs (10 different platings) incubated in CM (containing 25 mM K^+), a subpopulation of 72 neurons could be distinguished that maintained $[Ca^{2+}]_C$ at much higher levels (>600 nM) than the majority of CGCs (300–400 nM), but that nevertheless promptly decreased $[Ca^{2+}]_C$ to about 20 to 30 nM when CM was replaced with Locke's buffer and the extracellular K^+ ($[K^+]_E$) concentration was reduced from 25 to 5.6 mM (Fig. 1). Such neurons failed to buffer the $[Ca^{2+}]_C$ transients elicited by NMDA (see representative data in Fig. 1) or glutamate (data not shown). Because this subpopulation of neurons appears to have distinctly different properties, in the present study these neurons were singled out, and their data were

excluded when average responses, typical for the majority of CGCs, were calculated. This abnormal subpopulation of CGCs requires an additional, separate, characterization.

Substitution of Na^+ with NMG^+ Exacerbates Glutamate-Induced Destabilization of Ca^{2+} Homeostasis and Excitotoxicity. When the Na^+ in the extracellular medium of CGCs was replaced with NMG^+(NMG-Locke's), a 15-min exposure to glutamate (100 μM glutamate plus 10 μM glycine in the absence of Mg^{2+}) at 37°C resulted in a permanent destabilization of Ca^{2+} homeostasis (Fig. 2A). When the test of neuronal viability based on propidium iodide staining was performed 24 h after the neuronal challenge with glutamate, it was observed that many neurons were propidium iodide-negative in spite of evident morphological changes, such as a prominent shrinkage of the cell body (see white arrowheads in Fig. 2, A2 and E2). The lack of propidium iodide staining in such neurons complicated the quantitation of excitotoxicity. Obviously, 24 h after the challenge with glutamate the process of neurodegeneration was not yet accomplished. Therefore, additional experiments were performed in which neuronal viability was monitored for up to 70 h after the glutamate exposure (Fig. 2E). It was observed that of 182 neurons exposed to glutamate and NMG-Locke's, 115 died within the first 24 h, and an additional 45 during the next 46 h (Fig. 2F).

An analysis of whether the time of neuronal death is related to $[Ca^{2+}]_C$ changes during and after the glutamate exposure showed that the neurons that failed to decrease $[Ca^{2+}]_C$ levels within 20 min after glutamate withdrawal died within 19 h (compare the positions of neurons with high $[Ca^{2+}]_C$, red-colored in Fig. 3A4, with the positions of dead neurons in Fig. 3A6); all neurons that decreased $[Ca^{2+}]_C$ at least to the levels characteristic for CGCs incubated in CM were alive at that time (indicated with green arrowheads in Fig. 3A4). The neuron that buffered $[Ca^{2+}]_C$ sluggishly (indicated with white arrowhead in Fig. 3A4), was still alive after 19 h (Fig. 3A6), but was dead at 29 h (Fig. 3A7). Interestingly, a subpopulation of neurons begun to die after an even longer delay postglutamate; note two neurons that restored low $[Ca^{2+}]_C$ levels within 20 min after glutamate withdrawal (yellow arrowheads in Fig. 3A4), survived the first 29 h, but were dead at 44 h (Fig. 3A8). It appears that also in this case neuronal death was induced by the Ca^{2+} influx elicited by NMDA receptor activation because the CGCs that were exposed to glutamate in the presence of MK-801 survived for as long as 68 h (Fig. 3B). These results suggest that glutamate exposure may induce two Ca^{2+} influx-dependent but distinct mechanisms of neuronal death: the first one occurring within the first 24 h after the glutamate challenge and expressed in the impaired ability to restore basal Ca^{2+} levels in the cytoplasm, and the second one occurring during the next 24 h and triggered by the initial Ca^{2+} influx but not accompanied by a destabilization of Ca^{2+} homeostasis. Further work is necessary to characterize these two mechanisms on a molecular level.

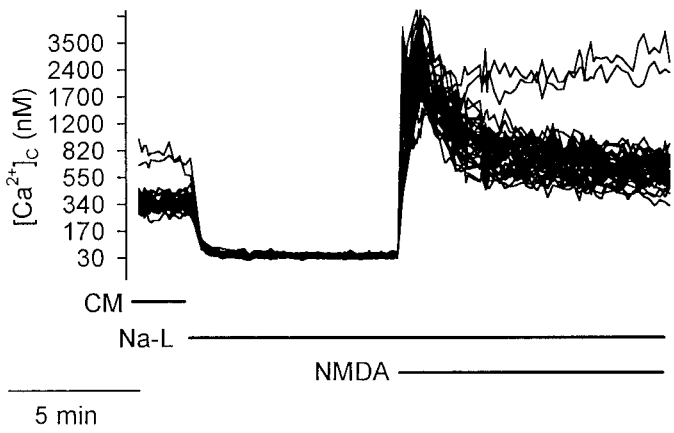

Fig. 1. Basal $[Ca^{2+}]_C$ levels and NMDA-induced $[Ca^{2+}]_C$ transients in CGCs. CGCs were loaded with fura-2 while incubated in a CM. As indicated by the bars, CM was replaced with Na-Locke's (Na-L) and then the cells were exposed to NMDA (300 μM NMDA + 10 μM glycine in the absence of Mg^{2+}). Shown are the $[Ca^{2+}]_C$ traces recorded from 39 individual neurons in a representative experiment. The two neurons that maintained very high $[Ca^{2+}]_C$ while incubated in CM are the same that failed to buffer the NMDA-induced $[Ca^{2+}]_C$ transient. Similar results were routinely observed in over 20 different preparations of CGCs.

In the overwhelming majority of CGCs, the glutamate-elicited $[Ca^{2+}]_C$ transient and excitotoxicity were completely blocked by 10 μM MK-801 (Fig. 3B), which indicates that the $[Ca^{2+}]_C$ transient and excitotoxicity result from the activation of the NMDA class of receptors. Only a single neuron was dead after 68 h (Fig. 3B7) but not 19 h (Fig. 3B6) after the exposure to glutamate plus MK-801. This happened to be the same neuron in which MK-801 failed to inhibit the glutamate-induced $[Ca^{2+}]_C$ transient (see arrowhead in Fig. 3B3). For the statistical relevance of this finding, more data have to be accumulated.

The data shown in Fig. 3 indicate that by using propidium iodide fluorescence, one can monitor the progress of neurodegeneration in vitro for an extended time, and relate the time of neuronal death to the severity of the glutamate-induced destabilization of Ca^{2+} homeostasis. Apparently, for up to 68 h propidium iodide by itself was not toxic to the neurons (Fig. 3B7). When PM was permeabilized with 0.01% Triton X-100, propidium iodide fluorescence was promptly observed in all CGCs (Fig. 3B8), which indicates that even as long as 68 h after the propidium iodide addition neuronal death could be detected.

When CGCs were challenged with glutamate while physiological Na^+ concentrations were present in the medium, following glutamate withdrawal, $[Ca^{2+}]_C$ returned to basal levels (Fig. 2C) and neuronal survival was greatly improved compared with the challenge with glutamate and NMG-Locke's: of 205 neurons exposed to glutamate and Na-Locke's, only 27 neurons died within 24 h and no additional neuronal death was detected for up to 70 h (Fig. 2, D and F). Interestingly, when CGCs were incubated in Na-Locke's and exposed to glutamate at room temperature but otherwise under identical experimental conditions, the glutamate-induced destabilization of Ca^{2+} homeostasis was more pronounced and the exposure was more excitotoxic (Kiedrowski, 1998). The temperature sensitive component(s) of the excitotoxic mechanism needs to be further characterized.

An enhancement of the NMDA-induced excitotoxicity by a Na-free buffer (Na^+ substituted with NMG^+) was reported earlier and interpreted to indicate that the increased excitotoxicity in the Na-free medium was due to a failure by the NaCaX to remove Ca^{2+} from the cytoplasm (Mattson et al., 1989), or due to an alleged glutamate release (Storozhevykh et al., 1998). An alternative and straightforward explanation needs to be considered, however: namely, that the replacement of Na^+ with a large extracellular cation, which cannot

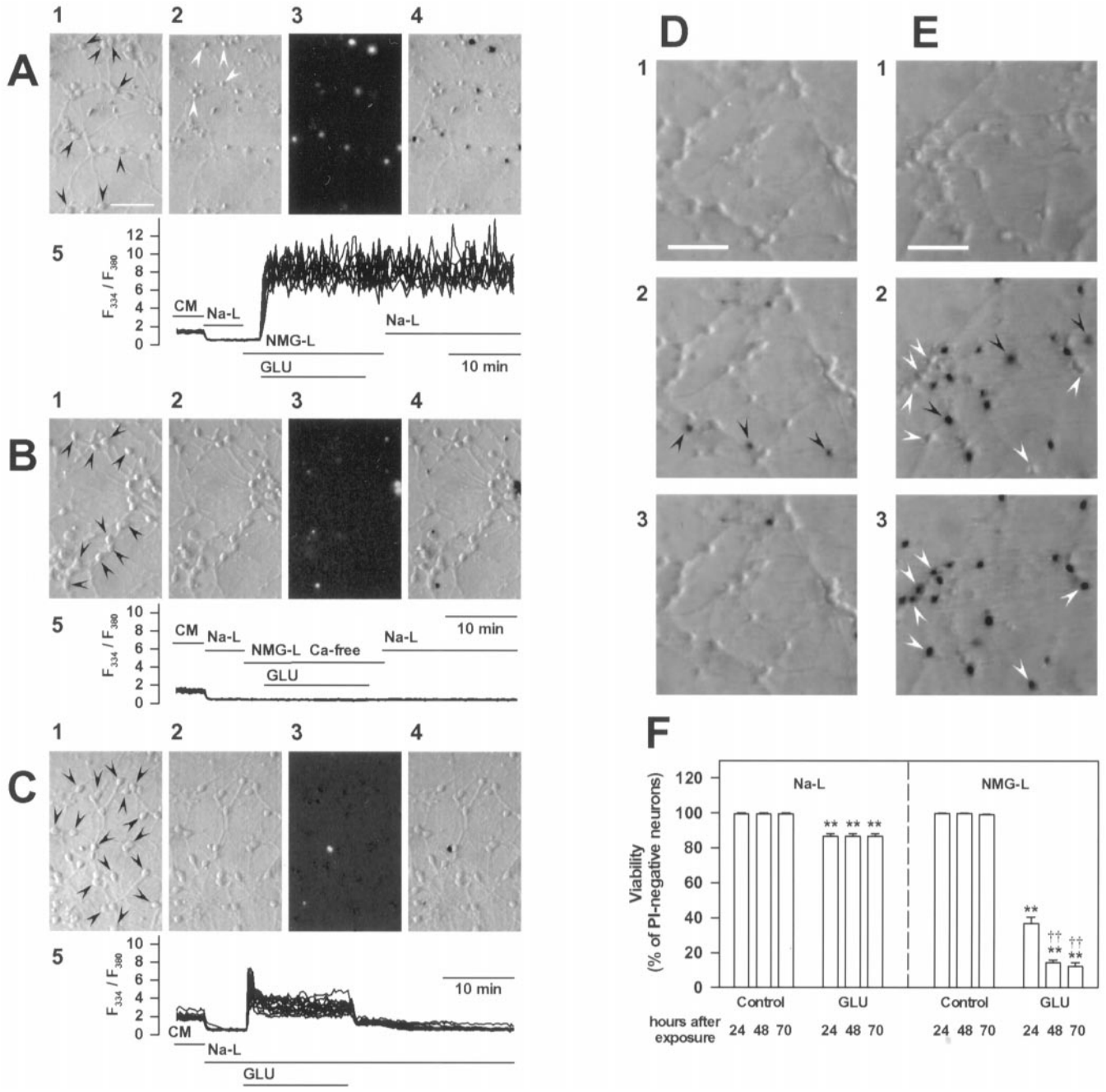

Fig. 2. Replacement of Na^+ with NMG^+ exacerbates the glutamate-induced destabilization of Ca^{2+} homeostasis and excitotoxicity. A, B, and C, relationships between Ca^{2+} homeostasis and neuronal survival. $[Ca^{2+}]_C$ was monitored in the CGCs indicated by the arrowheads in the oblique illumination images (A1, B1, and C1). Cells were exposed for 15 min at 37°C to 100 μM glutamate + 10 μM glycine (GLU) applied in a Mg-free Locke's buffer in which Na^+ was replaced with NMG^+ (NMG-L) when 1.3 mM extracellular Ca^{2+} was present (A), or absent (B), or in a buffer in which both Na^+ and Ca^{2+} were present (C). Cell viability was tested 24 h after the exposure by inspecting the same microscopic field (A2, B2, and C2). The cells with a damaged PM were identified using propidium iodide fluorescence (A3, B3, and C3). Using a procedure of digital subtraction described in *Materials and Methods*, the images of propidium iodide fluorescence were superimposed over the oblique illumination images (A4, B4, and C4). Note that negatives of the propidium iodide fluorescence are created, and therefore the previously bright spots become black. This procedure allows one to distinguish the "false" propidium iodide signals that represent cellular debris floating in the medium. Such debris is visible in images B3 and C3. A5, B5, and C5, show the GLU-induced $[Ca^{2+}]_C$ transients (F_{334}/F_{380} ratio) recorded from the cells indicated by the arrowheads in A1, B1, and C1, respectively. All experiments were repeated at least three times with similar results on different preparations of CGCs. Note that many neurons showing a profound morphological neurodegeneration (see arrowheads in A2) were still impenetrable to propidium iodide (A3), which may indicate that the process of PM disintegration in these neurons was not yet accomplished. D, E, F, progress of excitotoxicity in time. CGCs have been exposed for 15 min to GLU while incubated in Na-L (D) or NMG-L (E) ($[Ca^{2+}]_C$ was not monitored in this experiment). The superimposed images of oblique illumination and propidium iodide fluorescence D2, D3, E2, and E3 were constructed as described in *Materials and Methods* and illustrated in A–C. The scale bars shown in A1, D1, and E1 represent 50 μm. Average data from experiments analogous to those shown in D and E are presented in F. Data in F are means ± S.E.M. from three different dishes; each microscopic field was occupied by 53 to 85 neurons and a total of 190 to 239 neurons per each treatment was counted. Note that in many neurons that die following the exposure to GLU/NMG-L, the PM is impermeable for propidium iodide for at least 24 h (white arrowheads in E2 and E3). Note also that during the time course of the observation some neurons lost the propidium iodide stain due to disintegration (black arrowheads in D2 and E2). $^{**}p < .01$ compared with respective control, $\dagger\dagger p < .01$ compared with neuronal viability 24 h after the GLU/NMG-L challenge (one-way ANOVA followed by Newman-Keuls test).

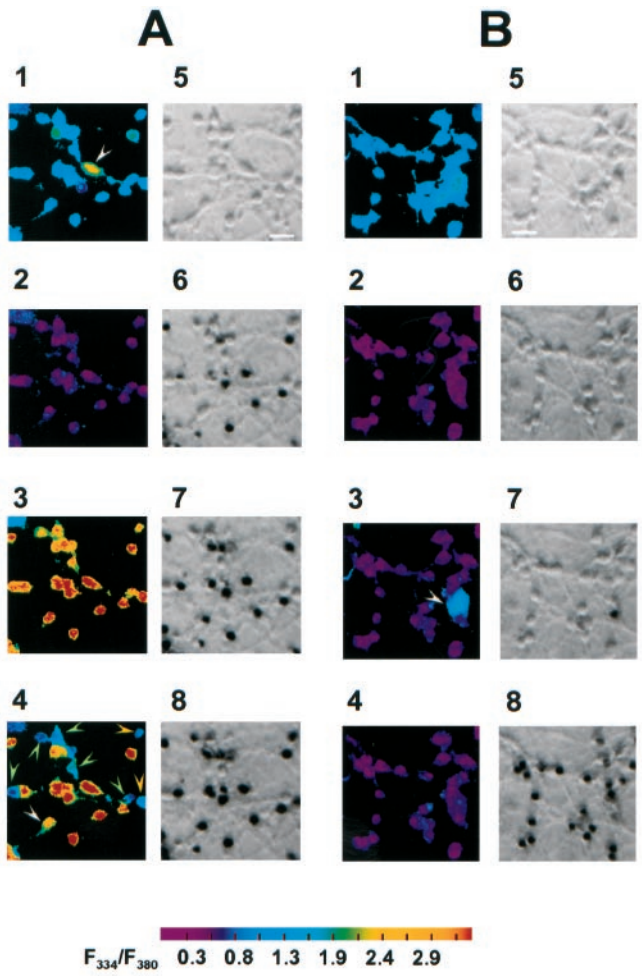

Fig. 3. The glutamate-induced Ca^{2+} influx and excitotoxicity in CGCs incubated in NMG-Locke's is blocked by MK-801. A, 1–4 show the F_{334}/F_{380} ratio images of fura-2 fluorescence from CGCs exposed to glutamate and NMG-Locke's the same way as described in Fig. 2 A. 5 and 6, show the oblique illumination images of the same cells at various times during the experiment. B, cells treated as in A but glutamate is applied with 10 μM MK-801. F_{334}/F_{380} ratio images were taken at the following times: A1 and B1, CGCs incubated in CM; the arrowhead points to the cell that represents the abnormal population of CGCs with high basal $[Ca^{2+}]_C$ described in the text; A2 and B2, 8 min after application of Na-Locke's; A3, 15 min after addition of Mg-free NMG-Locke's containing 100 μM glutamate and 10 μM glycine; B3, same as A3 but in the presence of MK-801; A4 and B4, 20 min after glutamate/glycine withdrawal, the cells incubated in Na-Locke's. Times at which the oblique illumination images were taken: A5 and B5, cells incubated in CM before the experiments; A6 and B6, 19 h after the challenge with glutamate, cells incubated in CM containing 10 μM propidium iodide; A7 and A8, 29 and 44 h after the challenge, respectively; B7, 68 h after the challenge, B8, same cells as shown in B7 but 2 min after addition of 0.01% Triton X-100. Cells indicated by arrowheads in A4 and B3 are described in the text. Scale bars in A5 and B5 represent 20 μm. Images 6, 7, and 8 of A and B are overlays of the propidium iodide fluorescence images over the oblique illumination images and were created as described in Fig. 2. Note that the CGCs that died first (A6) were those that failed to promptly restore low $[Ca^{2+}]_C$ following glutamate withdrawal (A4) and that MK-801 completely suppressed the glutamate-induced Ca^{2+} influx (B3) and excitotoxicity (B7) in the majority of CGCs.

permeate NMDA channels, prevents the PM depolarization elicited by Na^+ influx (Hösli et al., 1973). As a result, the electrochemical driving force for Ca^{2+} influx (CaDF), defined as the difference between E_m and the Ca^{2+} equilibrium potential, does not decay, or decays at a lower rate, which has to enhance Ca^{2+} influx via any Ca-permeable channel. To test the latter hypothesis, E_m and $[Ca^{2+}]_C$ were monitored simultaneously in CGCs exposed to NMDA.

Simultaneous Monitoring of E_m and $[Ca^{2+}]_C$. We have previously observed that activation of NMDA or kainate/α-amino-3-hydroxy-5-methyl-4-isoxazole propionic acid receptors in CGCs results in an elevation of $[Na^+]_C$ up to 60 mM or higher (Kiedrowski et al., 1994), which depolarizes the PM. While evaluating various means of monitoring E_m changes, I was concerned that a direct electrophysiological approach might not faithfully reflect the E_m changes characteristic for an intact neuron exposed to glutamate because the ionic content of the intracellular electrode, in particular high $[K^+]$, might obscure the glutamate-induced changes in $[Na^+]_C$ and $[K^+]_C$ characteristic for an intact neuron. Therefore, to monitor E_m for the purpose of this study, a noninvasive method was chosen, which makes use of the fluorescence of an E_m-sensitive dye, $DiBAC_4(3)$, an anionic fluorescent probe that accumulates in the cytoplasm of depolarized cells via a Nernst equilibrium-dependent uptake (Bräuner et al., 1984). $[Ca^{2+}]_C$ and E_m were monitored simultaneously according to the approach described by Laskey et al. (1992). Cells were first loaded with fura-2 and then exposed to 100 nM $DiBAC_4(3)$ (see *Materials and Methods* for details). After illumination at 334 and 380 nm to excite fura-2, there was no fluorescence emission by $DiBAC_4(3)$, and inversely, after 488 nm illumination to excite $DiBAC_4(3)$, there was no fluorescence emission by fura-2 (Fig. 4, B and C); therefore $[Ca^{2+}]_C$ and E_m could be monitored selectively in a single cell. PM depolarization was associated with a robust increase in $DiBAC_4(3)$ fluorescence, which was very intense in peripheral parts of cell bodies but virtually absent in the nuclear area (Fig. 4B). The apparent lack of $DiBAC_4(3)$ fluorescence in the nucleus of depolarized cells is consistent with earlier observations (Bräuner et al., 1984) and was confirmed using confocal microscopy (data not shown). Therefore, the peripheral parts of cell bodies were chosen to monitor $DiBAC_4(3)$ fluorescence as an index of E_m. To test the reliability of these E_m and $[Ca^{2+}]_C$ measurements, the E_m changes were imposed on CGCs by applying an unselective monovalent cation ionophore, gramicidin D (5 μM), and a Na- and Ca-free solution in which the K^+ concentration was changed from 163.2 to 3.6 mM by substituting K^+ with NMG^+. Under these conditions, 163.2 mM K^+ is expected to completely depolarize the PM, whereas 3.6 mM K^+ is expected to create a large, negative inside, K^+ diffusion potential. Repetitive applications of depolarizing pulses of 163.2 mM K^+ or hyperpolarizing pulses of 3.6 mM K^+ were associated with respective increases or decreases in $DiBAC_4(3)$ fluorescence intensity, indicative of the expected E_m changes (Fig. 4E). These changes in E_m failed to affect $[Ca^{2+}]_C$ in the majority of CGCs (Fig. 4E). In the above-described abnormal 4% subpopulation of CGCs with high $[Ca^{2+}]_C$ while incubated in the CM, however, the hyperpolarizing pulses of 3.6 mM K^+ were associated with $[Ca^{2+}]_C$ transients (data not shown), which, considering that the extracellular medium was Ca-free, represented Ca^{2+} release from intracellular stores. Similar Ca^{2+} transients were observed in cells that were about twice as large as CGCs and probably represented astrocytes (Fig. 4D). The lack of such intracellular Ca^{2+} release in the majority of CGCs confirms our earlier observations that intracellular Ca^{2+} stores in unstimulated CGCs are virtually de-

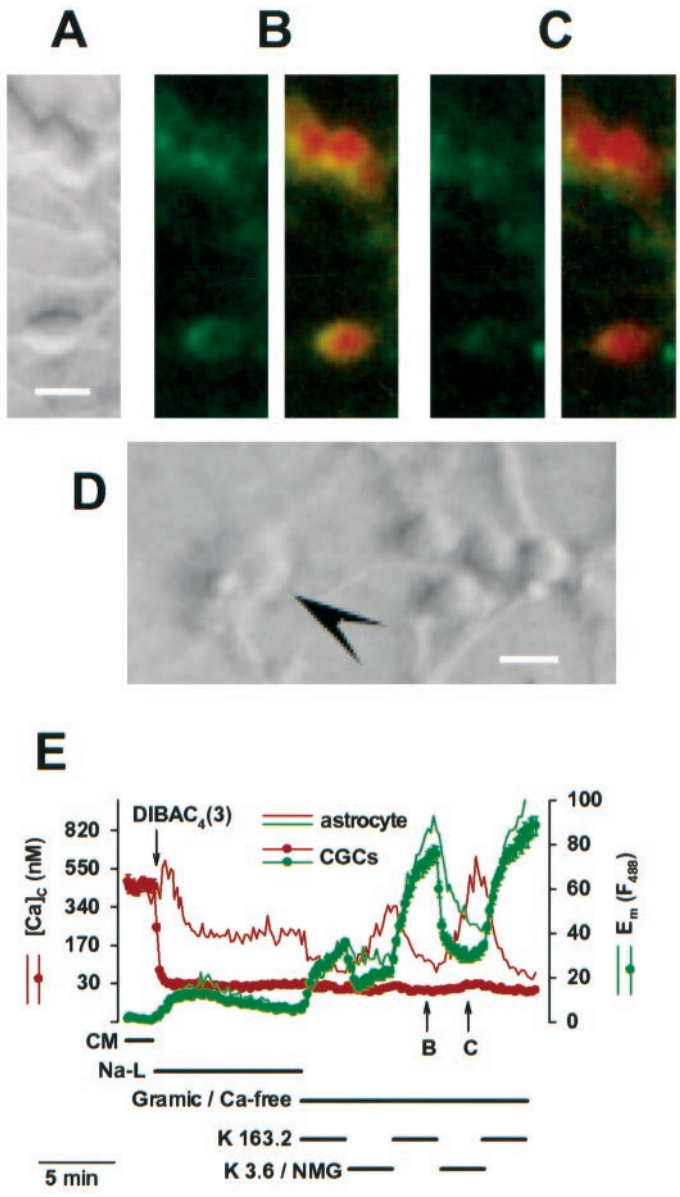

Fig. 4. The method of simultaneously monitoring $[Ca^{2+}]_C$ and E_m. A, a magnified portion of an oblique illumination image of granule neurons in which $[Ca^{2+}]_C$ and E_m were simultaneously monitored. The scale bar represents 10 μm. B, image of $DiBAC_4(3)$ fluorescence (left) and the overlay of $DiBAC_4(3)$ over fura-2 fluorescences (right) of CGCs shown in A depolarized with a solution containing 163 mM K^+ and 5 μM gramicidin. Note that the $DiBAC_4(3)$ fluorescence is intense in the peripheral parts of cell bodies. C, image of the same CGCs hyperpolarized with a solution containing 3.6 mM K^+, 159.6 mM NMG^+, and 5 μM gramicidin. Note that the $DiBAC_4(3)$ fluorescence in C is much less intense than in B. D, an oblique illumination image of a group of cerebellar granule cells and of a larger cell, indicated by the arrowhead, probably an astrocyte. $[Ca^{2+}]_C$ and E_m data from this presumed astrocyte are shown in E. The scale bar represents 10 μm. E, shown are average changes $\pm$ S.E.M. in $[Ca^{2+}]_C$ and in the $DiBAC_4(3)$ fluorescence intensity (F_{488}) monitored in 17 CGCs (including the three cells shown in A, B, and C) and in a single larger cell morphologically resembling an astrocyte (see D). The data were obtained in a single experiment representative of three such experiments performed on different preparations of CGCs. Arrows marked B and C indicate the times at which the images shown in B and C, respectively, were taken. The cells were incubated in CM, which was replaced with Na-Locke's containing 100 nM $DiBAC_4(3)$, and then the cells were exposed to Ca-free media containing 5 μM gramicidin D (Gramic/Ca-free) that either depolarized or hyperpolarized the PM. The depolarizing medium contained 5 μM gramicidin D, 3 mM EGTA, 134.2 mM K-gluconate, 25.4 mM KCl, 1 mM $MgCl_2$, 3.6 mM $KHCO_3$, 10 mM HEPES, pH 7.2,adjusted with Tris (K 163.2). In the hyperpolarizing medium $[K^+]_E$ was reduced to 3.6 mM by substituting K^+ with NMG^+ (K 3.6/NMG). Note that increases or decreases in the $DiBAC_4(3)$ fluorescence intensity faithfully reflect the expected changes in E_m. Note also that hyperpolarization of the PM in the presumed astrocyte, but not in CGCs, is associated with a $[Ca^{2+}]_C$ transient that represents Ca^{2+} release from an internal store. Similar $[Ca^{2+}]_C$ transients induced by PM hyperpolarization were observed in four other astrocytes.

pleted (Kiedrowski and Costa, 1995). The mechanism of the PM hyperpolarization-induced Ca^{2+} release from intracellular stores requires further investigation.

The E_m-dependent changes in $DiBAC_4(3)$ fluorescence intensity induced by a change in E_m were readily detectable; however, they occurred at very slow rates, which was expected (Bräuner et al., 1984). For example, application of 163.2 mM K^+ for as long as 3 min was not long enough to bring the $DiBAC_4(3)$ fluorescence to a steady plateau (Fig. 4E). Therefore, attempts to calibrate the $DiBAC_4(3)$ fluorescence for millivolts were abandoned. Instead, the $DiBAC_4(3)$ fluorescence was used as a relative measure of E_m: increase of the fluorescence meaning depolarization, decrease meaning hyperpolarization.

Substitution of Na^+ with NMG^+ Increases NMDA-Mediated Ca^{2+} Influx by Affecting E_m. The above-described approach of a simultaneous monitoring of $[Ca^{2+}]_C$ and E_m was used to test whether the NMG-induced destabilization of Ca^{2+} homeostasis (Figs. 2A and 3A) was caused by a dysfunction of the NaCaX or by a difference in E_m. Because in the overwhelming majority of CGCs incubated in NMG-Locke's glutamate elicited Ca^{2+} influx and excitotoxicity by activating NMDA receptors (Fig. 3 B), in subsequent experiments NMDA rather than glutamate was used as an excitatory stimulus. CGCs were exposed to NMDA (300 μM NMDA plus 10 μM glycine, in the absence of Mg^{2+}); for the first 2 min, NMDA was applied in a standard Locke's buffer containing Na^+ (Na-Locke's), and the expected $[Ca^{2+}]_C$ transient and depolarization of the PM promptly occurred (Fig. 5A). Then Na^+ was replaced with Li^+ or NMG^+, neither of which supports the NaCaX, but the remaining components of the previous solution were not changed. If the destabilization of Ca^{2+} homeostasis observed in CGCs exposed to glutamate when Na^+ is replaced with NMG^+ is caused by an inhibition of Ca^{2+} extrusion via the NaCaX, a replacement of Na^+ with Li^+ should yield an effect similar to that obtained by replacement of Na^+ with NMG^+. The switch from Na^+ to NMG^+ affected $[Ca^{2+}]_C$ and E_m differently, however, than the switch from Na^+ to Li^+ (Fig. 5A). In the presence of Ca^{2+}, NMG^+ elicited a robust increase in $[Ca^{2+}]_C$, and transiently hyperpolarized the PM; in the absence of Ca^{2+}, the NMG-dependent hyperpolarization persisted for as long as it was studied (Fig. 5A, lower). By contrast, when Na^+ was replaced with Li^+, NMDA depolarized the PM similarly as if Na^+ were present (Fig. 5A, lower), but $[Ca^{2+}]_C$ decreased, within 5 min, to significantly lower levels, i.e., 360 $\pm$ 8 nM in the presence of Li^+ (72 cells in four experiments) versus 665 $\pm$ 22 nM in the presence of Na^+ (74 cells, four experiments), respectively ($P < .001$, Mann–Whitney rank sum test; see Fig. 5A, upper for representative data).

Because the $[Ca^{2+}]_C$ data may represent Ca^{2+} influx as well as Ca^{2+} redistribution between the cytoplasm and the organelles, such as mitochondria and/or endoplasmic reticu-

lum, the NMDA-elicited $^{45}Ca^{2+}$ accumulation was also monitored under similar experimental conditions; the $^{45}Ca^{2+}$ accumulation data provide complementary information that characterizes the amount of Ca^{2+} that enters the cells. As shown in Fig. 5B, in a dose-dependent manner NMG^+ potentiated, whereas Li^+ inhibited, the NMDA-elicited $^{45}Ca^{2+}$ accumulation. From these data, it can be inferred that NMG^+ enhances and Li^+ inhibits the NMDA-elicited Ca^{2+} influx.

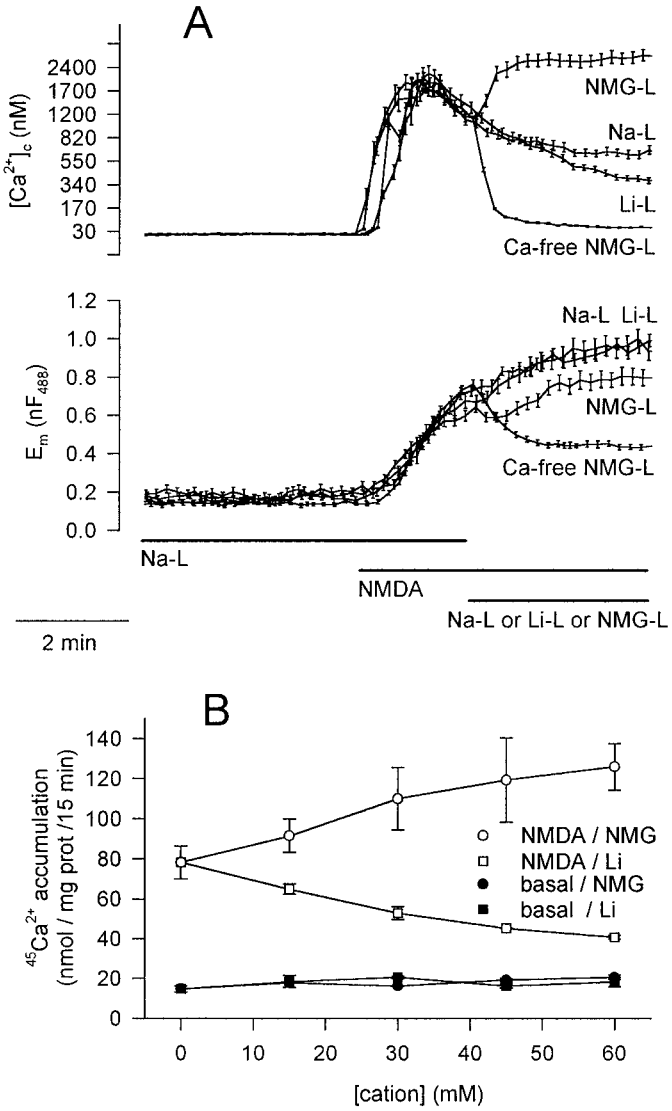

Fig. 5. Replacement of Na^+ with NMG^+ during neuronal exposure to NMDA hyperpolarizes the PM and stimulates Ca^{2+} influx. A, effects of NMG^+ and Li^+ on $[Ca^{2+}]_C$ (upper) and on E_m (lower) in CGCs exposed to NMDA; NMDA (300 μM NMDA + 10 μM glycine, Mg-free medium), Li-L (Na-free Locke's buffer, Na^+ replaced with Li^+). Data are the means ± S.E.M. from about 20 neurons in each experiment and were reproduced four times using two different preparations of CGCs. B, substitution of Na^+ with NMG^+ enhances NMDA-elicited $^{45}Ca^{2+}$ accumulation, but substitution of Na^+ with Li^+ has the opposite effect. $^{45}Ca^{2+}$ accumulation was measured as described in *Materials and Methods* in CGCs exposed for 15 min to 300 μM NMDA + 10 μM glycine applied in Mg-free Locke's buffers supplemented with the indicated concentrations of Li^+ (NMDA/Li) or NMG^+ (NMDA/NMG); Na^+ concentration was, respectively reduced to maintain osmoticity. To measure the basal $^{45}Ca^{2+}$ accumulation in the presence of Li^+ (basal/Li) or NMG^+ (basal/NMG), NMDA and glycine were omitted and 1 mM Mg^{2+} + 10 μM MK-801 were added to the medium. Data are the means ± S.E.M. from three experiments on three different preparations of CGCs.

These results can be interpreted to indicate that the mechanism of the NMDA plus NMG^+-induced neuronal overload with Ca^{2+} involves PM hyperpolarization and a consequent increase in the CaDF. Although E_m in CGCs exposed to NMDA in the presence of Li^+ changed similarly as in the presence of Na^+, there was an additional inhibition of the NMDA-induced Ca^{2+} influx by Li^+. This result may be related to the fact that Li^+ does not support the reverse operation of the NaCaX (Hilgemann, 1989), which contributes significantly to the NMDA-elicited Ca^{2+} influx in cultured neurons (Kiedrowski et al., 1994; Hoyt et al., 1998). It has to be noted, however, that the Ca^{2+}/Ca^{2+} exchange mode of the NaCaX, which is potently stimulated by extracellular Li^+ (Blaustein, 1977; Slaughter et al., 1983; DiPolo and Beaugé, 1990), may also contribute to the inhibitory effect of Li^+ on the NMDA-induced Ca^{2+} influx. Discrimination between Li^+ effects on the Ca^{2+}/Ca^{2+} exchange versus the Na^+/Ca^{2+} exchange mode in CGCs exposed to NMDA requires further work.

Relationships among E_m, $[Ca^{2+}]_C$, and pH_C. Because NMG^+, in contrast to Li^+, does not support the operation of the NaHX (Aronson, 1985), one might speculate that a cytoplasmic acidification, caused by a tonic inhibition of NaHX by NMG^+ (Raley-Susman et al., 1991), might affect Ca^{2+} homeostasis and contribute to the observed effects of substituting of Na^+ with NMG^+ versus Li^+. To test whether this is the case, the effects of Li^+ or NMG^+ on NMDA-induced changes in $[Ca^{2+}]_C$ and pH_C were measured simultaneously using the Ca^{2+}- and the pH-sensitive fluorescent dyes fura-2 and BCECF, respectively (see *Materials and Methods* for details). Basal pH_C in CGCs incubated in a standard Locke's buffer was 7.04 ± 0.01 (n = 340), which is consistent with previous observations (Raley-Susman et al., 1991; Hartley and Dubinsky, 1993; Irwin et al., 1994). While performing a simultaneous calibration of fura-2 and BCECF data in situ, it was observed that when pH_C dropped below 7.0, the maximal F_{334}/F_{380} ratio of fura-2 (R_{max}) progressively decreased (Fig. 6 A). It appears that a drop of pH_C below 7.0 affects the fura-2 fluorescence properties and, therefore, the in situ calibration of fura-2 performed at a pH_C of about 7.2 to 7.4 is not valid when pH_C drops below 7.0. Although in this report it was not attempted to correct for this artifact, the pH_C and the $[Ca^{2+}]_C$ data have been displayed simultaneously, and one can determine when the fura-2 F_{334}/F_{380} ratio might have been affected by the excessive drop in pH_C.

To test whether pH_C may directly affect $[Ca^{2+}]_C$, CGCs were exposed to 10 μM CCCP plus oligomycin (3 μg/ml). It was expected that CCCP, a protonophore, would disturb H^+ equilibria between the cytosol and the basic and acidic cytoplasmic organelles, as well as between the cytosol and the extracellular medium. Oligomycin was included to prevent hydrolysis of cytoplasmic ATP by mitochondrial ATP-ase (Budd and Nicholls, 1996). As shown in Fig. 6B, an application of CCCP plus oligomycin within 2 min caused a drop in pH_C by 0.72 ± 0.01 pH units (n = 47), whereas $[Ca^{2+}]_C$ remained unchanged. One may interpret this result as an indication that a drop in pH_C does not disturb Ca^{2+} homeostasis at least while $[Ca^{2+}]_C$ is maintained at basal levels.

To further explore the possibility of a link between pH_C and $[Ca^{2+}]_C$ regulation, how pH_C and $[Ca^{2+}]_C$ are affected by NMDA receptor activation in the presence of NMG^+ or Li^+

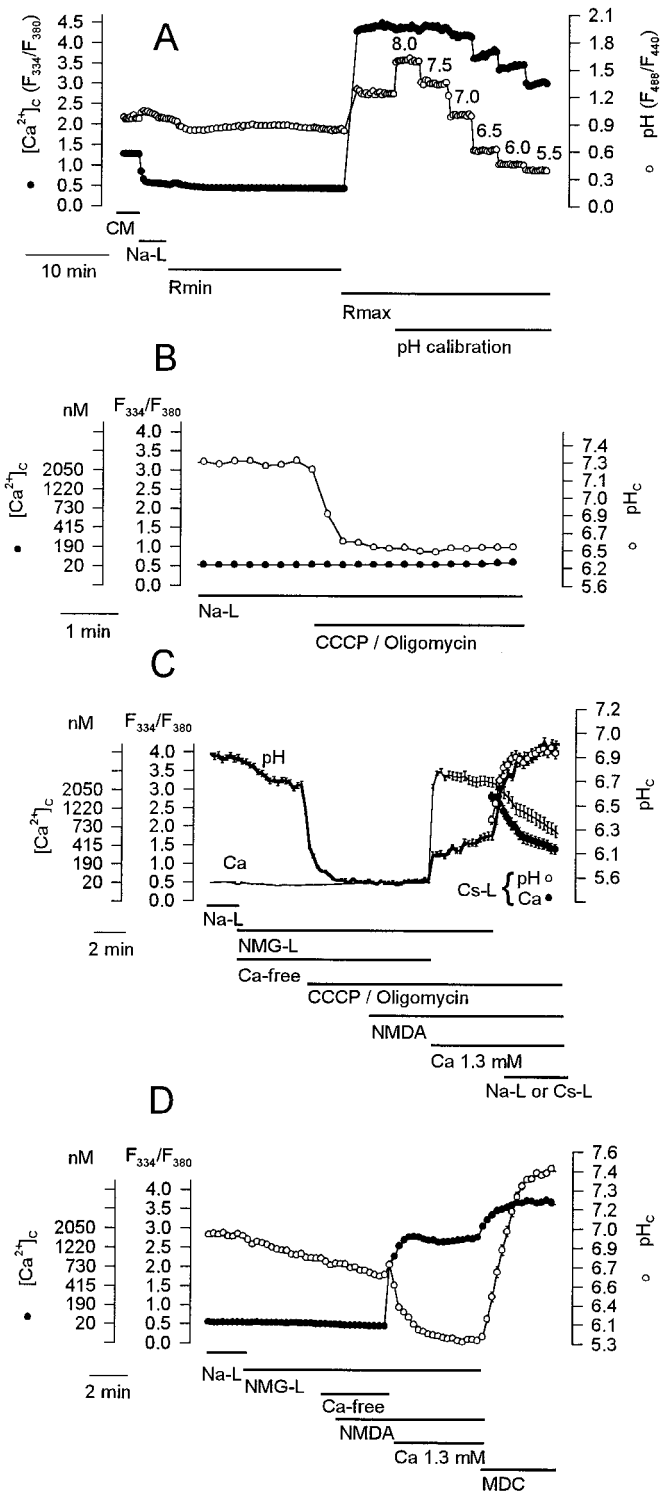

Fig. 6. Relations between pH_C and $[Ca^{2+}]_C$ in CGCs. A, simultaneous in situ calibration of fura-2 and BCECF fluorescences. Cells were exposed to CM, Na-L, and then to the buffers adjusting the fura-2 F_{334}/F_{380} ratio to the minimal (R_{min}), or maximal (R_{max}) value (see *Materials and Methods* for details). Then the plasma membrane was permeabilized for H^+ by application of 10 μM nigericin and 10 μM CCCP, and the pH of the R_{max} buffer was changed as indicated. The black ($[Ca^{2+}]_C$) and the white (pH_C) circles represent means from 56 neurons. S.E.M.s in this and several other panels of Figs. 6 and 7 are not visible because they are smaller than the areas covered by the symbols representing data points. Note that a drop in pH below 7.0 affects R_{max}. B, destabilization of $[H^+]$ equilibria between cytoplasmic organelles and cytosol and between cytosol and extracellular medium by application of 10 μM CCCP + oligomycin (3 μg/ml) affects pH_C but not $[Ca^{2+}]_C$. Data are the means from 47 neurons. The $[Ca^{2+}]_C$ values next to the abscissa in this as well as other panels were calculated based on an in situ calibration that was performed at pH 7.2. It has to be stressed, that in all cases when pH_C dropped below 7.0, such $[Ca^{2+}]_C$ values are underestimated, and are given only for the purpose of comparison with other experiments in which pH_C was not monitored. C, An influx of Na^+ or Cs^+ via the NMDA receptor channels rapidly removes the CCCP/oligomycin-induced acidification of the cytoplasm in CGCs incubated in NMG-L. Shown are overlapping data from two representative experiments testing the effects of Na^+ (60 neurons) or Cs^+ (56 neurons) on pH_C and $[Ca^{2+}]_C$. Because before the application of NMDA with Na-L or a Na-free Locke's buffer in which Na^+ was replaced with Cs^+ (Cs-L) similar patterns of pH_C and $[Ca^{2+}]_C$ changes were observed in both experiments, therefore, for clarity, the initial parts or the pH_C and $[Ca^{2+}]_C$ traces from the experiment in which Cs-L was applied (white and black circles) have been omitted. Data are the means ± S.E.M. Note that the application of Cs-L affects pH_C the same way as the application of Na-L does; in the presence of Cs-L, however, $[Ca^{2+}]_C$ decreases more rapidly. An interpretation of these results is given in the text. D, an NMDA-induced Ca^{2+} influx causes a more profound and more rapid drop in pH_C as compared with the drop in pH_C caused by an inhibition of the plasma membrane Na^+/H^+ exchanger with NMG^+. At the end of this experiment, CGCs were exposed to the MDC, which was Ca-free and contained 10 μM CCCP + 3 μg/ml oligomycin (for details see *Materials and Methods*). Data are the means from 38 neurons. Note that MDC causes a rapid alkalization of the cytoplasm.

was tested. It is well established that activation of NMDA receptors in a Ca-dependent manner acidifies the neuronal cytoplasm (Hartley and Dubinsky 1993; Irwin et al., 1994), and that a substitution of extracellular Na^+ with NMG^+ brings about a rapid further drop in pH_C, which has been interpreted as the result of a NaHX inhibition by NMG^+ (Hartley and Dubinsky, 1993). One has to consider, however, that the PM hyperpolarization induced by NMG^+ (Fig. 5A) may contribute to the acidification of the cytoplasm by two additional mechanisms: 1) an efflux of H^+ from the cytoplasm, as also an efflux of any other cation, is expected to be directly inhibited by PM hyperpolarization; and 2) PM hyperpolarization, by increasing the CaDF, increases Ca^{2+} influx, and is expected to enhance the mechanism by which Ca^{2+} influx alone affects pH_C (Irwin et al., 1994).

When extracellular Na^+ was replaced with NMG^+ under Ca-free conditions, pH_C decreased by 0.13 ± 0.01 pH units (n = 79), a subsequent application of CCCP plus oligomycin caused, similarly as in CGCs incubated in Na-Locke's, a rapid drop in pH_C, by 1.00 ± 0.02 pH units (compare Fig. 6, B and C). When NMDA was then added, neither $[Ca^{2+}]_C$ nor pH_C changed unless Ca^{2+} (1.3 mM) was added to the medium, which resulted in a rapid increase of pH_C, by 0.63 ± 0.03 pH units within 10 s, followed by a further, slow increase in pH_C, by 0.07 ± 0.02 pH units within the next 3 min; when, however, NMG^+ was then replaced with Na^+, a rapid restoration of basal pH_C was observed and $[Ca^{2+}]_C$ began to decrease (Fig. 6C). Based on the data shown in Fig. 5A, an obvious explanation of the Na- and also Ca-induced cytoplasmic alkalization is that the Na^+ influx via the NMDA receptor channel, and to a lesser degree the Ca^{2+} influx, depolarize the PM and annihilate the force that keeps protons in the cytoplasm, i.e., the highly negative E_m. One may insist however, that that Na-induced cytoplasmic alkalization is due to the activation of the NaHX rather than to the PM depolarization. To verify this claim, it was tested whether Cs^+, a cation that does not support the NaHX (Aronson, 1985) but permeates the NMDA receptor channel (Tsuzuki et al., 1994) and depolarizes the PM, can mimic the alkalizing effect of Na^+. As shown in Fig. 6C, Cs^+ reproduced the effect of Na^+,

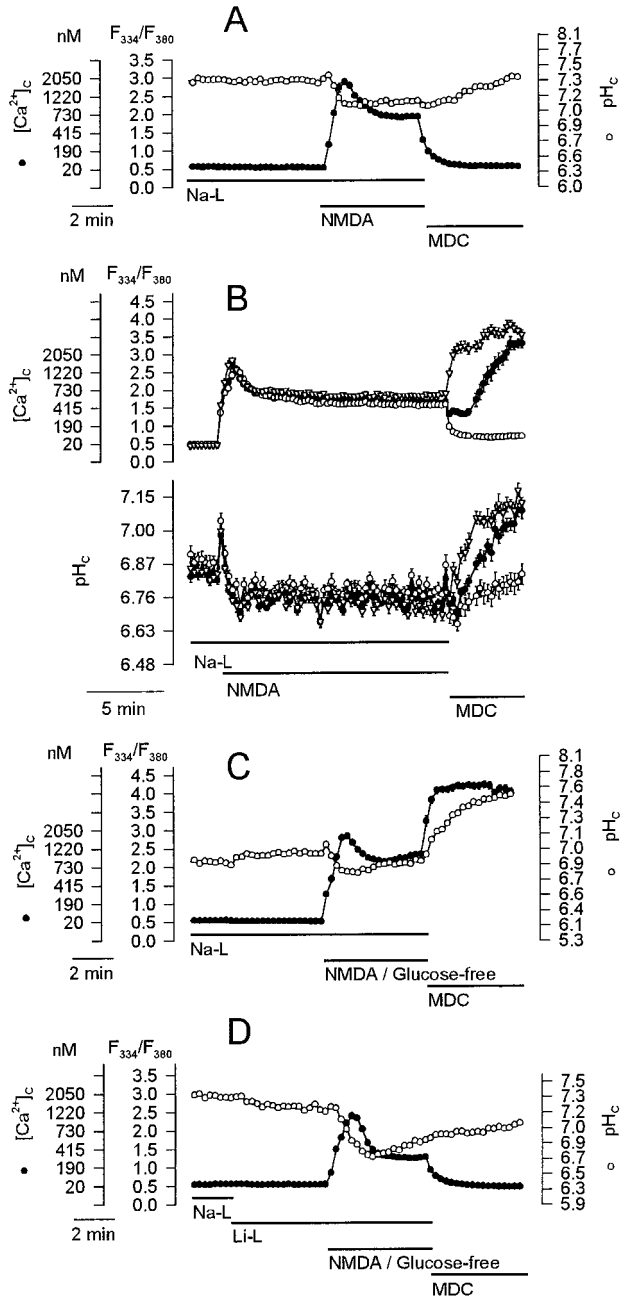

Fig. 7. Relationships between mitochondrial Ca^{2+} and pH_C in CGCs exposed to NMDA. A, in CGCs exposed to NMDA for 5 min only, MDC fails to elicit an increase in $[Ca^{2+}]_C$, which indicates that the exposure to NMDA was not associated with a mitochondrial Ca^{2+} overload. Data are the means from 43 neurons from a representative experiment. Compare with Fig. 6D and note that the NMDA-induced cytoplasmic acidification and the MDC-induced alkalization are much smaller in CGCs incubated in Na-L than in CGCs incubated in NMG-Locke. B, when MDC was applied to CGCs exposed to NMDA for 15 min, three populations of neurons could be distinguished based on the MDC effects on $[Ca^{2+}]_C$ and pH_C: 1) an instant increase in $[Ca^{2+}]_C$ and the most rapid alkalization of the cytoplasm (12 cells, △); 2) a delayed increase in $[Ca^{2+}]_C$ and a slower rate of cytoplasmic alkalization (16 cells, ●); and 3, a rapid drop in $[Ca^{2+}]_C$ not associated with any major change in pH_C (16 cells, ○). Data are the means ± S.E.M. from a representative experiment. C, when CGCs were deprived of glucose and exposed to NMDA for 5 min, MDC caused an instant increase in $[Ca^{2+}]_C$ and a rapid alkalization of the cytoplasm in all of CGCs. Data are the means from 46 neurons from a representative experiment. D, when the glucose-deprived CGCs were exposed to NMDA in the presence of Li-L, MDC caused a drop in $[Ca^{2+}]_C$ and failed to alkalize the cytoplasm. Data are the means ± S.E.M. from 57 neurons from a representative experiment.

which confirms the dominant role of PM depolarization in the mechanism of the here observed cytoplasmic alkalization, as well as the role of PM hyperpolarization in enhancing the Ca-dependent acidification of the cytoplasm.

Figure 6C also shows that after NMG^+ was substituted with Cs^+ or Na^+, $[Ca^{2+}]_C$ began to decrease, although NMDA, CCCP, and oligomycin were still present in the Mg-free extracellular medium, and that the rate of this decrease was faster when NMG^+ was substituted with Cs^+ than with Na^+. The mechanism of the decrease in $[Ca^{2+}]_C$ might include Ca^{2+} extrusion by the plasma membrane Ca^{2+} ATPase, or Ca^{2+} uptake to an internal store other than mitochondria, because mitochondria have already been depolarized with CCCP while the $[Ca^{2+}]_C$ decrease was observed. The faster rate of the $[Ca^{2+}]_C$ decrease in the presence of Cs^+ than in the presence of Na^+ may reflect the fact that cytoplasmic Na^+ but not Cs^+ activates the reverse mode of NaCaX operation, which counteracts the $[Ca^{2+}]_C$ drop.

When CGCs were exposed to NMG-Locke's in the presence of Ca^{2+}, pH_C begun to slowly decrease, and as Ca^{2+} was removed the rate of pH_C decrease remained unchanged (Fig. 6D). An application of NMDA under the Ca-free conditions also failed to affect the rate of the drop in pH_C. Only when 1.3 mM Ca^{2+} was introduced into the medium, was there a rapid drop in pH_C, by 0.97 ± 0.03 pH units (n = 38) within 2 min, which was accompanied by a steep rise in $[Ca^{2+}]_C$ to fura-2-saturating levels (Fig. 6D). These data confirm that the NMDA-induced drop in pH_C is a consequence of the NMDA-induced Ca^{2+} influx. The Ca^{2+} influx acidifies the cytoplasm via at least two concomitant mechanisms: 1) the activity of the plasma membrane Ca^{2+} pump, which exchanges intracellular Ca^{2+} for extracellular H^+ (Trapp et al., 1996); and 2) Ca^{2+} sequestration in mitochondria (discussed in the next section of this report).

Relationships among pH_C, Mitochondrial Ca^{2+} Overload, Plasma Membrane Na^+/Ca^{2+} Exchange Operation, and Energy Metabolism in CGCs Exposed to NMDA. Because glutamate excitotoxicity is associated with Ca^{2+} sequestration in mitochondria (Kiedrowski and Costa, 1995; Schinder et al., 1996; White and Reynolds, 1996), which has been causally linked to neuronal death (Stout et al., 1998), it was necessary to determine how substitution of extracellular Na^+ with NMG^+ versus Li^+ would affect the amounts of Ca^{2+} diverted to mitochondria. For this purpose, at the end of the 5-min period of monitoring $[Ca^{2+}]_C$ and pH_C in CGCs exposed to NMDA under various ionic conditions, the cells were treated with MDC, a Na-Locke's buffer that was Ca-free and glucose-free and contained 10 μM CCCP, 3 μg/ml oligomycin, and 10 μM MK-801. Any increase in $[Ca^{2+}]_C$ in response to the MDC application was expected to result from Ca^{2+} released from the depolarized cytoplasmic Ca^{2+} stores, including mitochondria.

In CGCs incubated in NMG-Locke's and exposed to NMDA, MDC caused a rapid alkalization of the cytoplasm by 1.9 ± 0.05 pH units (n = 38) within 2 min, i.e., to pH levels exceeding the basal pH_C; simultaneously, MDC caused an increase in the F_{334}/F_{380} ratio of fura-2 fluorescence (Fig. 6D). Although it is reasonable to expect that MDC would release Ca^{2+} from mitochondria and therefore increase $[Ca^{2+}]_C$, the $[Ca^{2+}]_C$ measured before the MDC additions was already at or close to the fura-2 saturating levels and it is unlikely that a further increase in $[Ca^{2+}]_C$ could be detected. Because the

MDC addition also caused a very marked increase in pH_C (Fig. 6D), which affects fura-2 fluorescence (Fig. 6A), the MDC-induced increase in the F_{334}/F_{380} ratio in these cells most likely represents a pH-dependent change in fura-2 fluorescent properties.

An application of NMDA to CGCs under control conditions, i.e., incubated in Na-Locke's, caused a modest drop in pH_C, by 0.2 ± 0.02 pH units (n = 84) within 2 min (Fig. 7A), and a typical $[Ca^{2+}]_C$ transient (compare the NMDA-induced $[Ca^{2+}]_C$ changes shown in Figs. 5A and 6D). It has to be noted, however, that just before NMDA induced a drop in the F_{488}/F_{440} ratio of BCECF fluorescence, a very short-lasting (less than 10 s) increase in this ratio was consistently observed (Fig. 7, A–C). To elucidate whether this increase in the F_{488}/F_{440} ratio represents a transient increase in pH_C and its mechanism, additional experiments are required.

MDC, when added to CGCs incubated in Na-Locke's and exposed to NMDA for 5 min, caused a prompt decrease of $[Ca^{2+}]_C$ and a slow increase of pH_C to basal levels (Fig. 7A). When, however, the exposure to NMDA was prolonged to 15 min, among 86 neurons tested, three populations of CGCs could be distinguished based on the effects of MDC on $[Ca^{2+}]_C$ and pH_C: 26% of neurons showed an instant increase in $[Ca^{2+}]_C$ and a rapid alkalization of the cytoplasm, which overshot the basal pH_C levels; in 40% of CGCs the MDC-induced increase in $[Ca^{2+}]_C$ occurred with a latency of about 1 min, and the MDC-elicited cytoplasmic alkalization occurred more slowly; in 35% of CGCs, following the MDC addition $[Ca^{2+}]_C$ dropped rapidly and pH_C began to slowly increase toward basal levels (Fig. 7C).

The latency in the MDC-induced increase in $[Ca^{2+}]_C$ that was observed in as many as 40% of CGCs exposed to NMDA for 15 min can be interpreted to indicate that the Ca^{2+} accumulated in mitochondria of these neurons was not present as free, ionized Ca^{2+} but as calcium bound by a mitochondrial Ca^{2+} buffer. Only after the mitochondrial $[Ca^{2+}]$ dropped to levels at which dissociation of free Ca^{2+} from this buffer was favorable, could Ca^{2+} be released from the mitochondria. One may expect that the formation of calcium phosphate in the mitochondrial matrix (Carafoli, 1987) participates in the mitochondrial Ca^{2+} buffering.

The fact that all neurons exposed to NMDA for 5 min (Fig. 7A) and 35% of neurons exposed to NMDA for 15 min (Fig. 7B) failed to show any increase in $[Ca^{2+}]_C$ after the MDC addition does not necessarily mean that the mitochondria of these neurons did not accumulate any Ca^{2+}. It may well be that the amounts of Ca^{2+} accumulated in these mitochondria were small and could be retained in the bound form even after the mitochondria were depolarized with MDC.

The rapid cytoplasmic alkalization induced by MDC in CGCs that have been exposed to NMDA and showed the prominent increase in $[Ca^{2+}]_C$ on the MDC addition (Figs. 6D and 7B) can be interpreted as follows. When $[Ca^{2+}]_C$ reaches the levels at which the rate of Ca^{2+} influx into mitochondria exceeds the rate of Ca^{2+} extrusion from mitochondria, the mitochondria start to accumulate Ca^{2+}, which depolarizes the inner mitochondrial membrane. To compensate for the mitochondrial membrane potential drop, regulatory mechanisms that extrude extra protons from the mitochondrial matrix are activated: for example, protons may be extruded by the mitochondrial ATPase at the expense of cytoplasmic ATP (Budd and Nicholls, 1996). The opposite scenario takes place when mitochondria are rapidly depolarized with MDC; the protons are then rapidly returned from the cytosol to the mitochondrial matrix whereas Ca^{2+} travels in the opposite direction. The overshooting of pH_C above basal values probably occurs because a fraction of the protons that have been extruded from the mitochondrial matrix to the cytosol in response to the mitochondrial Ca^{2+} influx is lost due to H^+ diffusion to the extracellular medium. As a result, at the time when MDC is applied, there is a deficit of protons in the cytosol, and when the protons return to the mitochondrial matrix, the cytosolic $[H^+]$ drops to lower than basal levels. Obviously, this interpretation of the data needs to be tested further.

When extracellular Na^+ was replaced with Li^+, the basal $[Ca^{2+}]_C$ remained unaffected but pH_C dropped within the first 2 min by 0.11 ± 0.01 pH units (n = 89) and then stabilized at this lower level. When NMDA was applied, a $[Ca^{2+}]_C$ transient occurred, and within 2 min pH_C dropped by 0.45 ± 0.02 pH units (n = 32); within the next 2 min of the exposure to NMDA, pH_C spontaneously recovered by 0.10 pH units. An application of MDC 5 min after the NMDA addition resulted in a rapid drop in $[Ca^{2+}]_C$ to basal levels and a slow increase of pH_C toward basal levels (data not shown; see, however, Fig. 7D for similar data obtained in CGCs deprived of glucose). The Li-Locke's-elicited drop in basal pH_C, as well as the more pronounced NMDA-induced drop in pH_C in CGCs incubated in Li-Locke's than in Na-Locke's, most likely reflects that Li^+ is less efficient than Na^+ in supporting the NaHX operation (Aronson, 1985).

Mitochondrial Ca^{2+} Overload in Energetically Challenged Neurons Results from Ca^{2+} Influx via Reverse Operation of Plasmalemmal NaCaX. Because the principal goal of in vitro studies of excitotoxicity is an understanding of the mechanisms of neurodegeneration characteristic of an ischemic brain, in which glutamate receptors are activated while the system is deprived of energy, it was of interest to examine how mitochondria would contribute to Ca^{2+} homeostasis and how pH_C would change under conditions of energy deprivation. To this end, $[Ca^{2+}]_C$ and pH_C were monitored in CGCs exposed to NMDA under glucose-free conditions. In such CGCs, following NMDA addition the $[Ca^{2+}]_C$ transient did not stabilize at a plateau level as observed when glucose was present (Fig. 7A) but after 2 to 3 min started to increase and during the 5th min of exposure $[Ca^{2+}]_C$ approached 1040 ± 57 nM, n = 46 (Fig. 7C); the steady increase in $[Ca^{2+}]_C$ was more clearly visible when the exposure to NMDA was longer than 5 min (data not shown). The pH_C changes in the majority of CGCs exposed to NMDA for 5 min were not affected by glucose deprivation (compare Fig. 7, A and C); however, glucose deprivation dramatically changed the effect of MDC addition on $[Ca^{2+}]_C$ and pH_C. When MDC was applied, $[Ca^{2+}]_C$ abruptly increased to fura-2 saturating levels, and this was accompanied by a rapid cytoplasmic alkalization that overshot the basal pH_C levels in 46 of 49 neurons (Fig. 7C). Note that the opposite result was observed in CGCs exposed to NMDA in the presence of glucose (Fig. 7A). In only three of 49 glucose-deprived neurons MDC caused a decrease in $[Ca^{2+}]_C$ accompanied by only a slight increase in pH_C (data not shown).

The effects of glucose deprivation on the NMDA-induced mitochondrial Ca^{2+} load and on pH_C changes were also studied in CGCs incubated in Li-Locke's. Based on the data

shown in Fig. 5, it was expected that Li^+ would inhibit the NaCaX-dependent fraction of the NMDA-induced Ca^{2+} influx. Indeed, in CGCs incubated in a glucose-free Li-Locke's, the NMDA-induced Ca^{2+} transient stabilized at a steady plateau level of 300 ± 7 nM (n = 57), which was three times lower than in CGCs incubated in Na-Locke (compare Fig. 7, C and D). When MDC was applied, $[Ca^{2+}]_C$ promptly dropped to basal levels, and a decrease in the rate of the cytoplasmic alkalization was observed (Fig. 7D), which is in dramatic contrast to the result observed in CGCs incubated in Na-Locke's under otherwise identical conditions (compare Fig. 7, C and D).

These results can be interpreted to indicate that when NMDA receptors are activated in the presence of Li^+, the NMDA-induced Ca^{2+} influx is limited because the reverse mode of NaCaX operation is inactive. Because the Na- or Li-induced depolarization of the PM decreases the CaDF, the subsequent Ca^{2+} influx directly via NMDA receptor channels as well as voltage-gated Ca^{2+} channels is very limited, and Ca^{2+} homeostasis can be maintained, for at least 15 min, without overloading mitochondria with Ca^{2+}. By contrast, the PM depolarization favors the reverse mode of operation of the NaCaX, which in CGCs incubated in Na-Locke's and exposed to NMDA appears to be the major source of the Ca^{2+} that overloads mitochondria and leads to neuronal death (Kiedrowski, 1999).

Because in CGCs incubated in Li-Locke's and exposed to NMDA Ca^{2+} did not overload mitochondria, one can envision that Li^+ might have a direct inhibitory effect on the mitochondrial Ca^{2+} influx. This possibility cannot be reconciled, however, with the data shown in Fig. 7D. If the mitochondrial Ca^{2+} uptake were indeed inhibited by Li^+ during the NMDA-exposure, $[Ca^{2+}]_C$ should be greatly elevated, which was not observed. Therefore, it appears that the proposed explanation, i.e., inhibition of the reverse NaCaX by Li^+, which is sufficient to explain all the data, remains valid.

NMDA Elicits a Ca-Dependent K^+ Efflux. From Fig. 5A (bottom) it is apparent that when all extracellular Na^+ was replaced with NMG^+, NMDA was still able to depolarize the PM, provided that Ca^{2+} was present in the medium. A possible mechanism might involve a Ca-dependent collapse of the K^+ concentration gradient across the PM, because the NMDA receptor channels are permeable to K^+ (Mayer and Westbrook, 1987; Tsuzuki et al., 1994). For this to be considered a valid explanation, one has to demonstrate first that the K^+ concentration gradient indeed collapses. To test this possibility, $[K^+]_C$ were measured using a K^+-sensitive fluorescent dye, PBFI (Minta and Tsien, 1989). The suitability of PBFI as a probe to measure $[K^+]_C$ was tested by monitoring PBFI fluorescence in CGCs exposed to glutamate. When glutamate was applied to CGCs incubated in Na- Locke's, no decrease in the F_{334}/F_{380} ratio of PBFI fluorescence was observed (Fig. 8A). Such an outcome might be caused by the poor selectivity of PBFI for K^+ over Na^+. The in vitro determined dissociation constant (K_d) of PBFI for K^+ is 8 mM and for Na^+ is 21 mM (Minta and Tsien, 1989), therefore, one may expect only a small change in PBFI fluorescent properties when intracellular K^+ is replaced by Na^+. Indeed, as soon as Na^+ was substituted with Li^+, an ion of low affinity for PBFI, K_d = 380 mM (Minta and Tsien, 1989), a prompt decrease was observed in the F_{334}/F_{380} ratio (Fig. 8A), which indicates an efflux of K^+ plus Na^+ from the cells and a simultaneous influx of Li^+. Using the in situ calibration as shown in Fig. 8A, the K_d of PBFI for K^+ was calculated as being 17.5 ± 0.8 mM (29 experiments on seven different preparations of CGCs). Due to this high affinity of PBFI for K^+, when $[K^+]_C$ exceeded 100 mM, PBFI was practically saturated with K^+, and changes in $[K^+]_C$ could not be detected unless $[K^+]_C$ dropped to 80 mM or lower.

In CGCs incubated in a Na-free Locke's buffer in which Na^+ was substituted with Li^+, NMDA caused a rapid and almost complete collapse of the K^+ concentration gradient across the PM, which was blocked by 10 μM MK-801 (Fig. 8B). When the $[K^+]_E$ was changed during the NMDA exposure, $[K^+]_C$ promptly adjusted to the new $[K^+]_E$ and remained at this level even after the Na^+/K^+ ATPase was inhibited with 1 mM ouabain (Fig. 8C). These data indicate that the opening of the NMDA receptor channels causes K^+ efflux and Li^+ influx, which continue until the concentration gradients of these ions across the PM completely collapse. Such dramatic loss of K^+ from the cytoplasm probably does not occur when physiological Na^+ concentrations are present in the medium, allowing normal operation of the Na^+/K^+ ATPase. When Na^+ is substituted with Li^+, the Na^+/K^+ ATPase cannot pump K^+ and Li^+ against their concentration gradients because Li^+ binds to both Na^+ and K^+ recognition sites of the enzyme (Hemsworth et al., 1997). As a result, the complete collapse of the Li/K concentration gradient across the PM is just a matter of time.

Although physiological changes in $[K^+]_C$ are not reflected in the PBFI fluorescence of cells incubated in Na-free media, this method can be used to explain the mechanism of the PM depolarization when Na^+ is replaced with NMG^+. As shown in Fig. 8D, under these conditions, the glutamate-elicited K^+ efflux occurred at a much lower rate and only in the presence of Ca^{2+} (Fig. 8D). This Ca-dependent drop in $[K^+]_C$ was slow and steady (Fig. 8D), and was blocked by MK-801 (not shown); by contrast, stepwise increases in extracellular Li^+ concentrations caused rapid drops of $[K^+]_C$ to lower and lower plateau levels (Fig. 8E).

These results can be interpreted to indicate that when all extracellular Na^+ is replaced with NMG^+, the activation of NMDA receptors in the absence of Ca^{2+} causes a K^+ efflux that is immediately curtailed by the PM hyperpolarization (Fig. 5A lower). In the presence of Ca^{2+}, this hyperpolarization is counteracted by a depolarizing Ca^{2+} influx, and therefore, $[K^+]_C$ continues to decrease (Fig. 8D). It appears that the different effects of Ca^{2+} and Li^+ on the kinetics of K^+ efflux (Fig. 8, D and E) occur because Ca^{2+} is buffered in the cytoplasm (Carafoli, 1987) but Li^+ is not. As a result, the Li^+ influx leads to a rapid equilibration of extracellular and intracellular Li^+ concentrations, followed by an arrest of the K^+ efflux due to the stabilization of E_m at a new K^+ equilibrium potential. In contrast, $[Ca^{2+}]_C$ does not equilibrate promptly with the extracellular Ca^{2+} concentration because of the cytoplasmic Ca^{2+} buffering. Although the extracellular Ca^{2+} concentration is only 1.3 mM, the supply of Ca^{2+} is virtually unlimited, because in vitro there is a vast excess of extracellular over intracellular volume. As a result, the Ca^{2+} influx via NMDA receptor channels compensates for the hyperpolarization caused by the K^+ efflux, and K^+ continues to flow away. Eventually, the K^+ concentration gradient across the PM collapses (Fig. 8D), which is reflected by the PM depolarization (Fig. 5A, lower). It should be noted that the

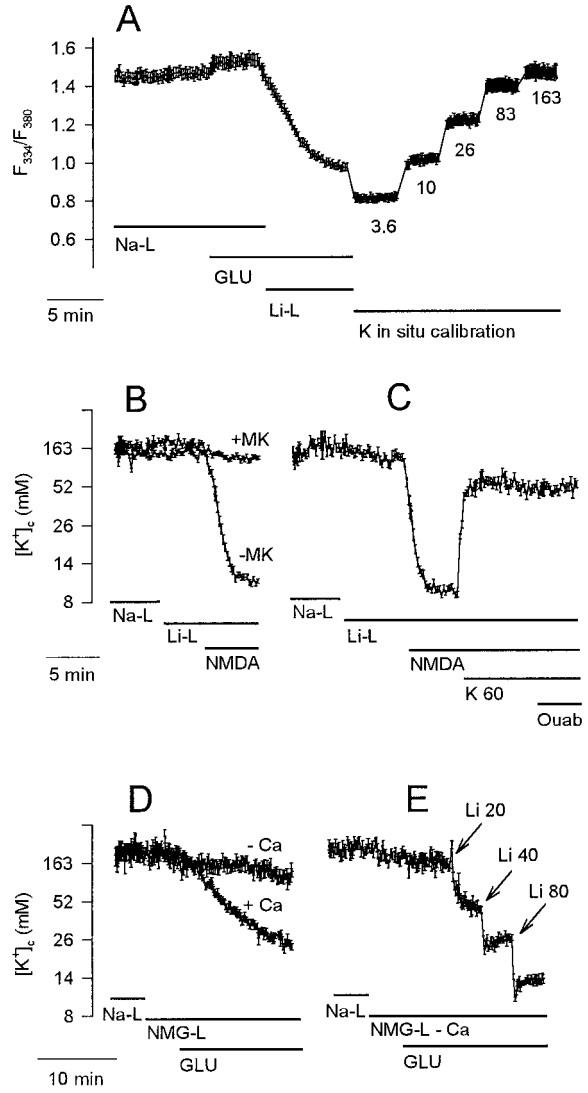

Fig. 8. $[K^+]_C$ in CGCs exposed to glutamate. A, method of monitoring $[K^+]_C$ using PBFI. CGCs loaded with PBFI (see *Materials and Methods* for details) were exposed to 100 μM glutamate + 10 μM glycine under Mg-free conditions (GLU) as described in Fig. 2. At the end of the experiment, $[K^+]_C$ was calibrated in situ using 5 μM gramicidin D and buffers containing the indicated K^+ concentrations (see *Materials and Methods* for details). Data are the means ± S.E.M. from 40 neurons. Note that glutamate failed to decrease the F_{334}/F_{380} ratio when applied in the presence of Na^+, but a prompt decrease in the F_{334}/F_{380} ratio was observed when Na^+ was replaced with Li^+, which reflects the fact that PBFI has a high affinity for K^+ and Na^+, but not for Li^+. B, NMDA-elicited K^+ efflux is blocked by MK-801 (MK). CGCs were exposed to NMDA, as described in Fig. 5, in the presence or absence of 10 μM MK-801. Data are the means ± S.E.M. from about 40 neurons in each experiment. C, when Na^+ is replaced with Li^+, $[K^+]_C$ in CGCs exposed to NMDA adjusts to ambient K^+ concentrations. In CGCs exposed to NMDA as in B, the $[K^+]_E$ was increased from 5.6 mM to 60 mM (K 60), followed by the addition of 1 mM ouabain (Ouab). Data are the means ± S.E.M. from 26 neurons. Note that the addition of ouabain failed to affect $[K^+]_C$, which indicates that the K^+ pumping by Na^+/K^+ ATPase was already inhibited by Li^+ alone. D, when Na^+ is replaced with NMG^+, glutamate elicits a slow and Ca-dependent K^+ efflux from CGCs. CGCs were exposed to 100 μM glutamate + 10 μM glycine under Mg-free conditions (GLU) in the presence of 1.3 mM Ca^{2+} (+ Ca) or in the absence of Ca^{2+} (− Ca). Data are the means ± S.E.M. from 28 to 37 neurons. E, additions of Li^+ to CGCs exposed to glutamate under Na-free (NMG^+ substitution) and Ca-free conditions rapidly reduce $[K^+]_C$ to steady-state levels. CGCs were exposed to GLU as described in D. The arrows indicate when Li^+ concentration was increased from 0 to 20, 40, or 80 mM (the NMG^+ concentration was appropriately reduced). Data are the means ± S.E.M. from 34 neurons.

monitoring of such a depolarization in an electrophysiological approach might be problematic; in that case, the K^+ concentration gradient would not collapse as long as the large excess of K^+ present in the intracellular electrode could prevent the drop in $[K^+]_C$.

The following concluding remarks can be made based on the data presented in this report:

1) The NMDA-induced and Na-dependent depolarization of the PM may be considered as a physiological regulatory mechanism via which the NMDA-elicited Ca^{2+} influx is restricted.

2) The NMDA-induced depolarization of the PM suppresses direct Ca^{2+} influx via the NMDA receptor channel but not the influx mediated by the reverse NaCaX. When cellular energy reserves are low and can no longer efficiently support Ca^{2+} extrusion, the reverse NaCaX is the dominant source of the Ca^{2+} that accumulates in mitochondria, and may play an important role in excitotoxicity.

3) The NMDA-elicited Na^+ influx may have a dual role in excitotoxicity: a protective role due to the depolarization-dependent decrease in the CaDF, and a promoting role due to Ca^{2+} influx via the reverse operation of the NaCaX. The final Ca^{2+} load that determines whether neurons will live or die (Hartley et al., 1993; Eimerl and Schramm, 1994) may depend on the balance between these two opposite effects. This balance may vary depending on the duration of the neuronal exposure to NMDA: i.e., the Na-dependent depolarization may be protective if the exposure is short-lasting, but when the exposure is prolonged, the NaCaX reversal may enhance Ca^{2+} influx to toxic levels. It has to be emphasized that these two opposite mechanisms may be differently balanced in various neuronal populations, which might explain why a 15-min exposure to 100 μM glutamate at 37°C under physiological Na^+ concentrations is excitotoxic to cortical neurons (Hoyt et al., 1998), whereas CGCs tolerate such exposure well (Fig. 2C).

4) The enhancement of the NMDA-induced Ca^{2+} influx observed in neurons incubated in Na-free media, where Na^+ is substituted with large cations that poorly, if at all, permeate the NMDA channel, occurs due to an increase in the CaDF. The CaDF is elevated because K^+ efflux via the NMDA channel hyperpolarizes the PM. The same consideration applies not only to Ca^{2+} but also to other cations, such as for example Mg^{2+}. Under physiological conditions, Mg^{2+} blocks the NMDA channel in a voltage-dependent manner (Mayer et al., 1984; Nowak et al., 1984), but when Na^+ is substituted with NMG^+, Mg^{2+} permeates the NMDA channel with abnormal ease (Stout et al., 1996).

Additionally, the NMG-induced enhancement of Ca^{2+} influx may also result from a lack of competition between Na^+ and Ca^{2+} for the NMDA channel. Further study is needed to evaluate the importance of such competition.

5) The NMDA-induced decrease in pH_C results from Ca^{2+} influx, which activates two pH_C decreasing mechanisms: a) Ca^{2+} extrusion by the plasmalemmal Ca^{2+}/H^+ pump, and b) Ca^{2+} sequestration in mitochondria. The NMDA-induced depolarization of the PM in the presence of Na^+, Li^+, or Cs^+ facilitates H^+ efflux to the extracellular medium, which counteracts the above-mentioned acidification. When the PM depolarization is prevented by NMG^+, H^+ is retained in the cytoplasm, and, as a result, the NMDA-induced acidification

is enhanced. Of course, the fact that the NaHX is inhibited under such conditions also contributes to the drop in pH_C.

6) In the absence of monovalent cations in the extracellular medium, NMDA elicits a Ca-dependent, slow depolarization of the PM, which results from the collapse of the K^+ concentration gradient across the PM.

Acknowledgments

I am grateful to Drs. J.-M. Mienville and N. Smalheiser for thoughtful discussions and to N. Grazulis for help in preparing the manuscript.

References

Aronson PS (1985) Kinetic properties of the plasma membrane Na^+-H^+ exchanger. *Annu Rev Physiol* **47:**545–560.

Blaustein MP (1977) Effects of internal and external cations and of ATP on sodium-calcium and calcium-calcium exchange in squid axons. *Biophys J* **20:**79–111.

Bräuner T, Hulser DF and Strasser RJ (1984) Comparative measurements of membrane potentials with microelectrodes and voltage-sensitive dyes. *Biochim Biophys Acta* **771:**208–216.

Budd SL and Nicholls DG (1996) A reevaluation of the role of mitochondria in neuronal Ca^{2+} homeostasis. *J Neurochem* **66:**403–411.

Carafoli E (1987) Intracellular calcium homeostasis. *Ann Rev Biochem* **56:**395–433.

Choi DW (1987) Ionic dependence of glutamate neurotoxicity. *J Neurosci* **7:**369–379.

DiPolo R and Beaugé L (1990) Asymmetrical properties of the Na-Ca exchanger in voltage-clamped, internally dialyzed squid axons under symmetrical ionic conditions. *J Gen Physiol* **95:**819–835.

Eimerl S and Schramm M (1994) The quantity of calcium that appears to induce neuronal death. *J Neurochem* **62:**1223–1226.

Grynkiewicz G, Poenie M and Tsien RY (1985) A new generation of Ca^{2+} indicators with greatly improved fluorescence properties. *J Biol Chem* **260:**3440–3450.

Hartley Z and Dubinsky JM (1993) Changes in intracellular pH associated with glutamate excitotoxicity. *J Neurosci* **13:**4690–4699.

Hartley DM, Kurth MC, Bjerkness L, Weiss JH and Choi DW (1993) Glutamate receptor induced $^{45}Ca^{2+}$ accumulation in cortical cell culture correlates with subsequent neuronal degeneration. *J Neurosci* **13:**1993–2000.

Hemsworth PD, Whalley DW and Rasmussen HH (1997) Electrogenic Li^+/Li^+ exchange mediated by the Na^+-K^+ pump in rabbit cardiac myocytes. *Am J Physiol* **41:**C1186–C1192.

Hilgemann DW (1989) Giant excised cardiac sarcolemmal membrane patches: Sodium and sodium-calcium exchange currents. *Pfleugers Arch* **415:**247–249.

Hilgemann DW, Collins A and Matsuoka S (1992) Steady-state and dynamic properties of cardiac sodium-calcium exchange. Secondary modulation by cytoplasmic calcium and ATP. *J Gen Physiol* **100:**933–961.

Hoyt KR, Arden SR, Aizenman E and Reynolds IJ (1998) Reverse Na^+/Ca^{2+} exchange contributes to glutamate-induced intracellular Ca^{2+} concentration increases in cultured rat forebrain neurons. *Mol Pharmacol* **53:**742–749.

Hösli L, Andrès PF and Hösli E (1973) Ionic mechanisms underlying the depolarization of L-glutamate on rat and human spinal neurones in tissue culture. *Experientia* **29:**1244–1247.

Irwin RP, Lin S-Z, Long RT and Paul SM (1994) *N*-methyl-D-aspartate induces a rapid, reversible, and calcium dependent intracellular acidosis in cultured fetal rat hippocampal neurons. *J Neurosci* **14:**1352–1357.

Jones KH and Senft JA (1985) An improved method to determine cell viability by simultaneous staining with fluorescein diacetate-propidium iodide. *J Histochem Cytochem* **33:**77–79.

Kasner SE and Ganz MB (1992) Regulation of intracellular potassium in mesangial cells: A fluorescence analysis using the dye, PBFI. *Am J Physiol* **262:**F462–F467.

Kiedrowski L (1998) The difference between mechanisms of kainate and glutamate excitotoxicity in vitro: Osmotic lesion versus mitochondrial depolarization. *Restor Neurol Neurosci* **12:**71–79.

Kiedrowski L (1999) Elevated extracellular K^+ concentrations inhibit NMDA-induced Ca^{2+} influx and excitotoxicity. *Mol Pharmacol*, in press.

Kiedrowski L, Brooker G, Costa E and Wroblewski JT (1994) Glutamate impairs neuronal calcium extrusion while reducing sodium gradient. *Neuron* **12:**295–300.

Kiedrowski L and Costa E (1995) Glutamate-induced destabilization of intracellular calcium concentration homeostasis in cultured cerebellar granule cells: Role of mitochondria in calcium buffering. *Mol Pharmacol* **47:**140–147.

Laskey RE, Adams DJ, Cannell M and Vanbreemen C (1992) Calcium entry-dependent oscillations of cytoplasmic calcium concentration in cultured endothelial cell monolayers. *Proc Natl Acad Sci USA* **89:**1690–1694.

Mattson MP, Guthrie PB and Kater SB (1989) A role for Na^+-dependent Ca^{2+} extrusion in protection against neuronal excitotoxicity. *FASEB J* **3:**2519–2526.

Mayer ML and Westbrook GL (1987) The physiology of excitatory amino acids in the vertebrate central nervous system. *Progr Neurobiol* **28:**197–276.

Mayer ML, Westbrook GL and Gurthie PB (1984) Voltage-dependent block by Mg^{2+} of NMDA responses in spinal cord neurons. *Nature* (*Lond*) **309:**261–277.

Minta A and Tsien RY (1989) Fluorescent indicators for cytosolic sodium. *J Biol Chem* **264:**19449–19457.

Nowak L, Bregestovski P, Ascher P, Herbert A and Prochiantz A (1984) Magnesium gates glutamate activated channels in mouse central nervous system. *Nature* (*Lond*) **307:**462–465.

Pinelis VG, Segal M, Greenberger V and Khodorov BI (1994) Changes in cytosolic sodium caused by a toxic glutamate treatment of cultured hippocampal neurons. *Biochem Mol Biol Int* **32:**475–482.

Raley-Susman KM, Cragoe EJ Jr, Sapolsky RM and Kopito RR (1991) Regulation of intracellular pH in cultured hippocampal neurons by an amilioride-insensitive Na^+/H^+ exchanger. *J Biol Chem* **266:**2739–2745.

Rothman SM (1985) The neurotoxicity of excitatory amino acids is produced by passive chloride influx. *J Neurosci* **5:**1483–1489.

Schinder AF, Olson EC, Spitzer NC and Montal M (1996) Mitochondrial dysfunction is a primary event in glutamate neurotoxicity. *J Neurosci* **16:**6125–6133.

Slaughter RS, Sutko JL and Reeves JP (1983) Equilibrium calcium-calcium exchange in cardiac sarcolemmal vesicles. *J Biol Chem* **258:**3183–3190.

Storozhevykh T, Grigortsevich N, Sorokina E, Vinskaya N, Vergun O, Pinelis V and Khodorov B (1998) Role of Na^+/Ca^{2+} exchange in regulation of neuronal Ca^{2+} homeostasis requires re-evaluation. *FEBS Lett* **431:**215–218.

Stout AK, Li-Smerin Y, Johnson JW and Reynolds IJ (1996) Mechanisms of glutamate-stimulated Mg^{2+} influx and subsequent Mg^{2+} efflux in rat forebrain neurones in culture. *J Physiol (Lond)* **492:**641–657.

Stout AK, Raphael HM, Kanterewicz BI, Klann E and Reynolds IJ (1998) Glutamate-induced neuronal death requires mitochondrial calcium uptake. *Nature Neurosci* **1:**366–373.

Tsuzuki K, Mochizuki S, Iino M, Mori H, Mishina M and Ozawa S (1994) Ion permeation properties of the cloned mouse epsilon 2/zeta1 NMDA receptor channel. *Mol Brain Res* **26:**37–46.

Trapp S, Lueckermann M, Kaila K and Ballanyi K (1996) Acidosis of hippocampal neurones mediated by a plasmalemmal Ca^{2+}/H^+ pump. *Neuroreport* **7:**2000–2004.

White RJ and Reynolds IJ (1996) Mitochondrial depolarization in glutamate-stimulated neurons: An early signal specific to excitotoxin exposure. *J Neurosci* **16:**5688–5697.

Send reprint requests to: Lech Kiedrowski, Ph.D., The Psychiatric Institute, 1601 W. Taylor St., Chicago, IL 60612. E-mail: lkiedr@psych.uic.edu